

Changes in water age during dry-down of a non-perennial stream

Co-author list: Logan J. Swenson^{1,2,*}, Sam Zipper^{1,*}, Delaney M. Peterson³, C. Nathan Jones³, Amy J. Burgin⁴, Erin Seybold¹, Matthew F. Kirk⁵, Camden Hatley^{1,2}

Affiliations:

1. Kansas Geological Survey, University of Kansas
2. Department of Geology, University of Kansas
3. Department of Biological Sciences, University of Alabama
4. Kansas Biological Survey-Center for Ecological Research, University of Kansas
5. Department of Geology, Kansas State University

* Corresponding authors: loganswenson@ku.edu, samzipper@ku.edu

Author ORCID IDs:

Swenson: 0000-0003-4981-3478

Zipper: 0000-0002-8735-5757

Peterson: 0000-0002-3444-4772

Jones: 0000-0002-5804-0510

Burgin: 0000-0001-8489-4002

Seybold: 0000-0002-0365-2333

Kirk: 000-0001-5562-7618

Hatley: 0000-0001-9840-2734

This is a non-peer-reviewed manuscript being submitted to Water Resources Research.

Key points:

- Stream isotopic composition was progressively enriched in $\delta^{18}\text{O}$ and $\delta^2\text{H}$ as the stream network dried.
- Stream isotopic enrichment is caused by evaporative effects and a decrease in surface water connectivity.
- Most streamflow was young water (stored in the subsurface < 3 months), with older and more variable water age as the stream network dried.

Abstract:

Non-perennial streams, which lack year-round flow, are widespread globally. Identifying the sources of water that sustain flow in non-perennial streams is necessary to understand their potential impacts on downstream water resources, and guide water policy and management. Here, we used water isotopes ($\delta^{18}\text{O}$ and $\delta^2\text{H}$) and two different modeling approaches to investigate the spatiotemporal dynamics of young water fractions (F_{yw}) in a non-perennial stream network at Konza Prairie (KS, USA) during the 2021 summer dry-down season, as well as over several years with varying hydrometeorological conditions. Using a Bayesian model, we found a substantial amount of young water (F_{yw} : 39.1 to 62.6%) sustained flows in the headwaters and at the catchment outlet during the 2021 water year, while 2015-2022 young water contributions estimated using sinusoidal models indicated smaller F_{yw} amounts ($15.3\% \pm 5.7$). Both modeling approaches indicate young water releases are highly sensitive to hydrological conditions, with streamwater shifting to older sources as the network dries. The shift in water age suggests a shift away from rapid fracture flow towards slower matrix flow that creates a sustained but localized surface water presence during late summer and is reflected in the annual dynamics of water age at the catchment outlet. The substantial proportion of young water highlights the vulnerability of non-perennial streams to short-term hydroclimatic change, while the late-summer shift to older water reveals a sensitivity to longer-term changes in groundwater dynamics. Combined, this suggests that local changes may propagate through non-perennial stream networks to influence downstream water availability and quality.

Plain Language Summary:

Non-perennial streams, which periodically dry, are common worldwide. Identifying the origin and age of water in non-perennial streams will help guide water policy and management strategies. We used water isotopes ($\delta^{18}\text{O}$ and $\delta^2\text{H}$), a common hydrologic tracer, to identify stream water sources and age during the 2021 summer dry-down period of a non-perennial watershed at the Konza Prairie (KS, USA) with two different statistical methods. We found that water sources and flowpaths changed as the stream network dried. Approximately half of summer streamflow is young water, meaning it took less than 3 months to travel from precipitation to the stream. However, as the summer progressed, streamwater shifted to older sources. We interpret this shift in the water age to indicate a shift in the source of water from rapid flowpaths early in the summer to slower flowpaths later in the summer, which sustain localized surface water during the driest parts of the year. Taken together, the substantial amount of young water highlights the vulnerability of non-perennial streams to short-term weather changes and longer-term changes in groundwater dynamics that can alter the quantity and quality of water flowing through non-perennial stream networks to ultimately influence downstream water availability and quality.

1. Introduction

Non-perennial streams, including intermittent and ephemeral streams that do not flow year-round (Busch et al., 2020), constitute more than half the global stream network length (Messenger et al., 2021), and are becoming more common worldwide due to water abstraction and climate change (Zipper et al., 2021; Sauquet et al., 2021; Trambly et al., 2021). Given their global prevalence and their shifts between aquatic (flowing) and terrestrial (dry) conditions, non-perennial streams can strongly influence the ecological health of river networks through regulation of biogeochemical cycles of nutrients and organic matter (Hale and Godsey, 2019; Zimmer and McGlynn, 2018) and local and downstream water quality and quantity (Gómez et al., 2017; Zimmer et al., 2022). Despite their importance, non-perennial streams are overlooked, undermonitored, and understudied relative to perennial streams (Krabbenhoft et al., 2022). However, growing recognition of their abundance has driven attempts to refine hydrological and ecological theories to account for the unique characteristics of non-perennial flow regimes (Shanafield et al., 2021; Allen et al., 2020; DelVecchia et al., 2022), particularly related to the patterns, dynamics, and drivers of stream drying (Price et al., 2021; Hammond et al., 2021).

While a growing number of contemporary studies have highlighted the important and unique role of non-perennial streams on watershed hydrologic and ecological function, management of and policy affecting these systems remains contested and unclear (Walsh and Ward, 2022). In the US, federal policy debates over non-perennial stream protections focus on “significant connectivity” between non-perennial streams and downstream ‘navigable’ waters (Alexander, 2015). Since 2015, three different Environmental Protection Agency rules have been used to define protections of non-perennial streams - resulting in repeated disagreement and reversal of protections (Ward et al. 2023). Definitions of protected waters have considered if they have a “significant nexus” (Clean Water Rule, 2015), if they are “relatively permanent” (Navigable Waters Protection Rule, 2020), or more recently with new US federal protections that allowed either the “relatively permanent standard” or “significant nexus standard” to classify protected waters (Revised Definition of “Waters of the United States”, 2023). However, the newly revised federal policy that expanded protections for non-perennial streams has already been overturned in the Supreme Court, leading to an uncertain future for non-perennial stream protection and management in the US (Liptak, 2023). Globally, this policy debate is mirrored in other regions. For example, in the European Union, the inclusion and protection of non-perennial streams in management frameworks is still emerging and varies widely between member countries (Leone et al., 2023). These policy debates highlight the need to better characterize the hydrology of non-perennial streams and quantify their impact on both local and downstream ecosystem function.

Quantifying the connection between non-perennial streamflow and water quality first requires an understanding of the origin of water in these streams and the timescales over which water is transmitted to the stream (Hrachowitz et al., 2016), which affects, for example, redox processes (Zarnetske et al., 2011) and mineral weathering rates (Maher, 2010). While previous studies have investigated temporal dynamics of water age in temporary rivers (von Freyberg et al., 2018; Gallart et al., 2020a; Sprenger et al., 2022; Lapides et al., 2022), they integrate age and source to a single measurement point at the watershed outlet, thereby failing to capture the potential variation in the spatial distribution of water within a network (Jensen et al., 2019; Botter and Durighetto, 2020). Thus, quantifying the within-network spatial and temporal evolution of water age and sources in non-perennial streams underpins our ability to predict the vulnerability of these systems to changes in groundwater dynamics and streamflow which are exacerbated by changing climate and human activities (Zipper et al., 2022; Datry et al., 2022). For example, understanding the source of late summer baseflow could direct nonpoint source pollution management activities to improve water quality. Ultimately, understanding the age and source of water in non-perennial streams can help determine when and how they will impact water quantity and quality in downstream waters (Zimmer et al., 2022).

To advance this understanding, our goal was to quantify the spatiotemporal variability in stream isotopic composition and water age, and infer changes in water source, during the dry-down of a non-perennial stream network at the Konza Prairie Biological Station (Kansas, USA). Specifically, we asked three questions: (1) How do streamwater isotopic compositions in non-perennial streams vary spatially and temporally? (2) What factors most strongly influence the distribution of isotopic compositions in non-perennial streams, and how do these factors vary through time? (3) What does this imply about the sources of water and their transit times sustaining streamflow?

We answered these questions using water isotopes ($\delta^{18}\text{O}$ and $\delta^2\text{H}$), a commonly applied hydrologic tracer for identifying water sources and modeling water age (Jasechko, 2019), using both a Bayesian unmixing model and a sinusoidal modeling approach to infer young water fractions over both time and space. We applied both models to isotopic samples that were collected through regular sampling at the watershed outlet, and also used the Bayesian approach for three spatially-dense synoptic campaigns throughout summer 2021 to evaluate both spatial and temporal dynamics in water age as the stream network dried. Finally, we investigated how young water releases from catchment storage are modulated by calculating discharge sensitivity of young water fractions with both Bayesian and sinusoidal models.

2. Data and Methods

2.1. Study Site

This study focuses on Kings Creek at the Konza Prairie Biological Station in the Flint Hills ecoregion of Kansas, USA (Figure 1). Konza Prairie is a native tallgrass prairie, part of the National Ecological Observatory Network (NEON) and is a Long Term Ecological Research (LTER) site. The terrain is merokarst with thin limestone units (1-2 m thick) interbedded with mudstone/shale units (2-4 m thick), and is characterized by flashy stream responses to precipitation events, preferential flow through conduits, and strong vertical heterogeneity (Sullivan et al., 2020; Vero et al., 2018; Macpherson 1996). The landscape is terraced with more resistant limestone units forming benches on hillslopes and knickpoints in stream channels, while less resistant mudstones erode to more gradual slopes (Costigan et al., 2015). Soils are predominantly silty-clay loams; however, bedrock commonly outcrops at the surface (Ransom et al., 1998). Soil profiles are deepest at the base of slopes (~2 m) and are thinnest on the ridges (<20-50 cm) (Ransom et al., 1998).

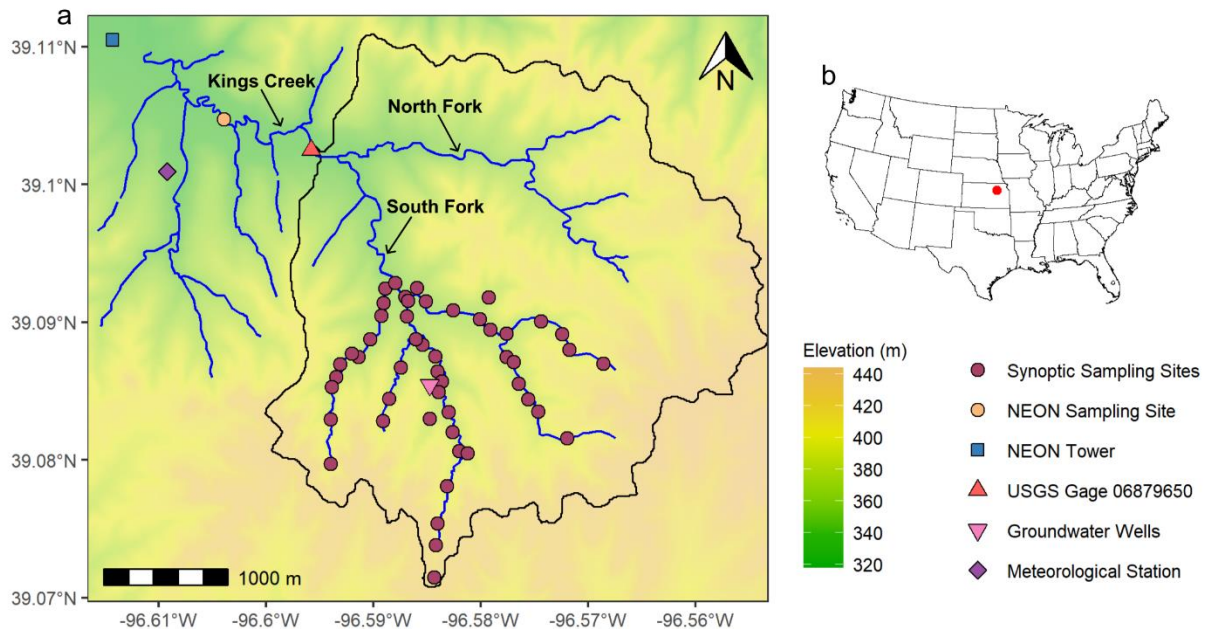


Figure 1. (a) Sampling sites and infrastructure along Kings Creek in the Konza Prairie, KS, USA. Stream isotopes were collected in the headwaters of the South Fork of Kings Creek (Synoptic Sampling Sites), while long-term samples were taken further downstream in Kings Creek (NEON Sampling Site). Precipitation isotopes were collected as composite samples from a wet deposition collector (NEON Tower). The outlet of the North and South Forks of Kings Creek has been monitored by the U.S. Geological Survey since 1979 (USGS Gage 06879650) with a drainage area of 1150 ha of tall grass prairie.

Note: The groundwater well nest is offset 50 m away from the stream to be visible. (b) Location of the Konza Prairie in the US.

The climate is mid-continental with cold, dry winters and warm, humid summers (Vero et al., 2018). Average annual precipitation is 835 mm, with ~75% of rainfall occurring between April and September, when vegetation is active and evapotranspiration rates are high (Hayden, 1998). Water lost to evapotranspiration is the primary fate of water, representing ~70% of rainfall (~600 mm under long-term conditions; Logan and Brunsell, 2015), and increases in evapotranspiration associated with woody vegetation encroachment have caused decreases in streamflow over the past four decades despite increases in precipitation (Sadayappan et al., 2023). Konza Prairie received 632 mm precipitation in the 2021 calendar year (76% of the annual average, Figure 2); however, it was unequally distributed throughout the year. Spring (March-April) was very wet (85 percentile of 30 year conditions) while the summer was very dry (2.5 percentile of 30 year conditions). 1150 ha of tall grass prairie is drained by Kings Creek, a fifth order stream which has been monitored by the U.S. Geological Survey (USGS) since 1979 (USGS gage 06879650). The Kings Creek network dries in many, but not all, years between approximately July and September due to a decrease in precipitation and increase in evapotranspiration (Costigan et al., 2015). Groundwater wells are screened in the Upper and Lower Eiss and Morrill limestone units (stratigraphic unit names), which past work found to contribute considerable amounts of groundwater to the stream at mid-elevations in the South Fork of Kings Creek via springs along the hillslopes and within the streambed (Hatley et al., 2022). Due to the karstic nature of these limestone units and well-developed but localized stream-aquifer connections, discharge and groundwater levels respond quickly to precipitation events, with the initial response typically occurring within 2 h of the event and peaking between 2.5 and 5 h afterwards (Hatley et al., 2022; Brookfield et al., 2016). Based on pressure responses and rising-head slug tests in the groundwater wells, the Upper Eiss Limestone appears to have slightly higher hydraulic conductivity than the Morrill Limestone (10^{-5} to 10^{-4} m d⁻¹ for the Upper Eiss compared to 10^{-5} to 10^{-3} m d⁻¹ for the Morrill), with both having greater hydraulic conductivity and stream connectivity than the Lower Eiss Limestone (10^{-8} to 10^{-5} m d⁻¹ for the Lower Eiss) (Figure 2; Barry, 2018; Pomes, 1995).

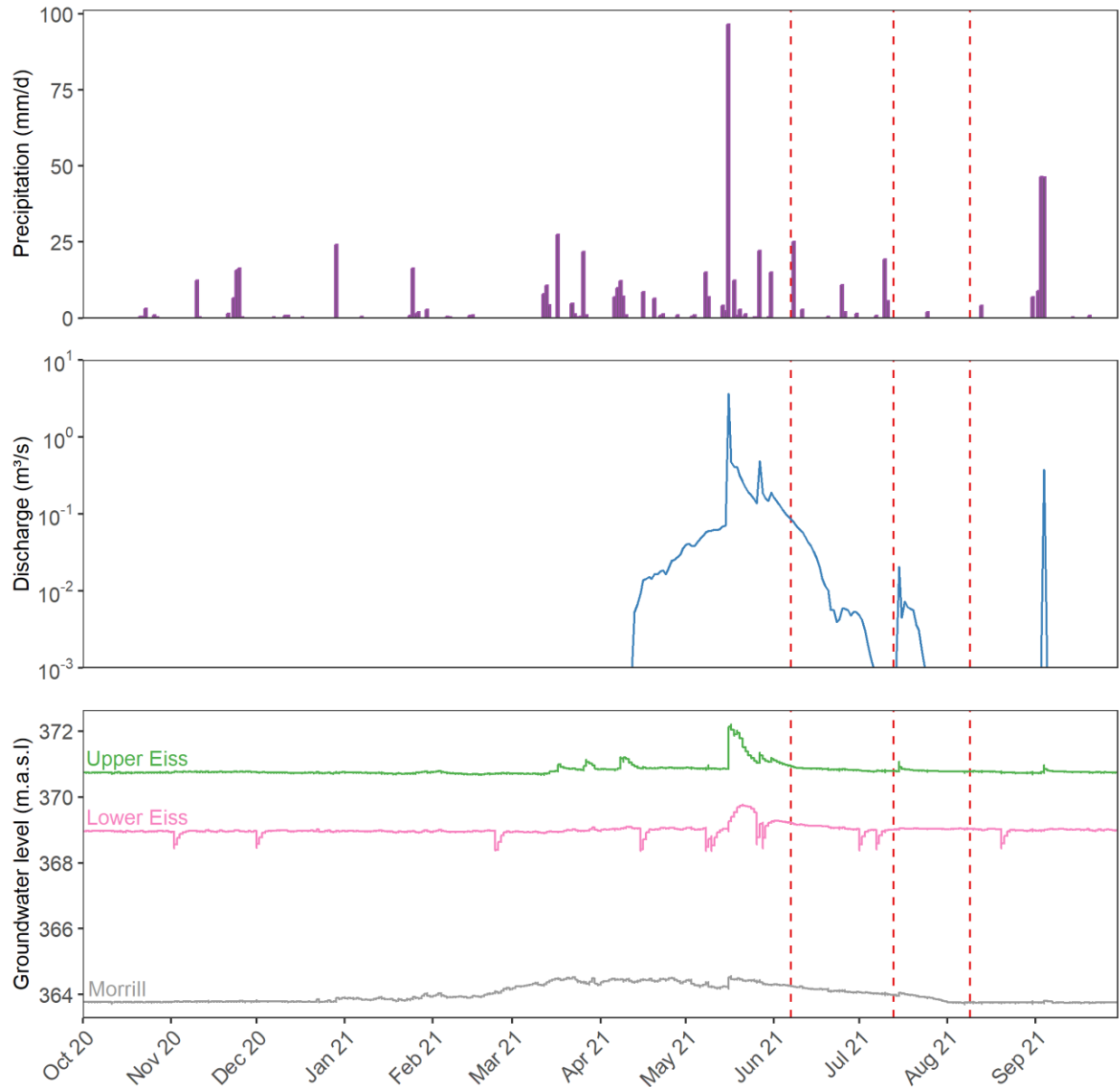


Figure 2. Timeseries of (a) precipitation, (b) discharge at USGS gage 06879650, and (c) groundwater levels at the Konza Prairie. Synoptic sampling events are shown as vertical dashed lines. Sharp declines in groundwater levels in the Lower Eiss occurred as a result of periodic sampling events and slow recovery in this low-conductivity unit.

2.2. Sampling Design & Ancillary Data

Water isotopes ($\delta^{18}\text{O}$ and $\delta^2\text{H}$) were collected on June 7th, July 13th, and August 9th (2021) as part of three spatially-distributed synoptic sampling campaigns designed to capture a range of surface water connectivity conditions during the dry-down of a non-perennial stream network. We identified 50

sampling sites spanning a range of drainage area and topographic wetness index, which have been previously shown to be significant predictors of flow permanence in non-perennial streams (Warix et al., 2021). A subset of the locations strategically targeted sites with long-term data, known springs, and other locations of interest (see supplemental section S1 for full details on the sampling design). The synoptic samples were collected only on the South Fork of Kings Creek, and the most downstream synoptic network sampling point represented a drainage of 531 ha. On each sampling date, we visited all 50 sampling sites and collected samples if water was present, along with ancillary information regarding the hydrologic conditions (i.e., whether the water was flowing or pooled and water temperature). A total of 77 distinct grab samples, excluding replicates, were obtained: 43 samples in June, 19 samples in July, and 15 samples in August. All samples were stored in 60-mL glass vials with conical inserts and capped without headspace to prevent isotopic fractionation. Samples were kept in dark and at room temperature (<20 °C) until analysis.

Additional data were compiled from the USGS, National Ecological Observatory Network (NEON), and the Konza Prairie Long Term Ecological Research (LTER) programs. Discharge in Kings Creek was obtained from USGS gage 06879650, which is ~1.6 km downstream from the most downstream point of our synoptic sampling (Figure 1). Composite precipitation isotopes were collected approximately every two weeks between November 2018 and January 2022 from a wet deposition collector at the NEON Tower, with a gap in collection from March 2020 to July 2020 during the onset of the COVID-19 pandemic (n = 51; Figure 1; NEON, 2022). The precipitation-sampling collectors meet International Atomic Energy Agency (IAEA) recommendations to prevent evaporation. In addition to the precipitation isotopes, stream isotopes were collected approximately every two weeks between October 2015 and January 2022 at the NEON Sampling Site (n = 146; Figure 1; NEON, 2022), which is ~1.1 km downstream of the USGS gage, and has a contributing area of 1306 ha. The USGS and NEON measurement points had substantially larger contributing areas, incorporating both the North and South Fork of Kings Creek, while the synoptic samples were only in the South Fork. NEON precipitation and stream isotopes were stored in dark, cool (<20 °C) conditions and analyzed at the SIRFER Lab at University of Utah. Daily precipitation amounts were recorded at the Konza Prairie Headquarters meteorological station (Figure 1; Nippert, 2022). Groundwater levels were logged at 5-min intervals in the Upper Eiss, Lower Eiss, and Morill limestone aquifers (Figure 1; Hatley et al., 2022). The meteorological and groundwater data collection networks are maintained by the Konza Prairie LTER program.

2.3. Lab Analysis

Surface water isotopes were measured using a cavity ring-down spectroscopic isotopic water analyzer (Picarro L2130-*i*, Picarro Inc., CA). In order to account for memory effects, each sample was run as six sub-samples. The first three sub-samples were used to equilibrate the cavity (and therefore were excluded from the analysis), whereas the last three sub-samples were averaged to calculate sample isotopic compositions. To account for instrument drift and precision, all samples were calibrated against internal secondary standards, which were run repeatedly every 6 samples. Internal secondary standards were calibrated against the IAEA primary standards for Vienna Standard Mean Ocean Water (VSMOW; $\delta^{18}\text{O} = 0.0\text{‰}$, $\delta^2\text{H} = 0.0\text{‰}$). Average instrument precision was calculated as 0.05‰ and 0.41‰ for $\delta^{18}\text{O}$ and $\delta^2\text{H}$ respectively based on the comparison of 41 total duplicate internal secondary standards. Isotopes values were reported in parts per thousand (‰) deviation relative to VSMOW:

$$\delta = (R_s/R_{\text{std}} - 1) * 1000$$

where R_s and R_{std} are the isotope ratio ($^2\text{H}/^1\text{H}$ or $^{18}\text{O}/^{16}\text{O}$) in the samples and standard (VSMOW) respectively (Craig, 1961).

Deuterium excess (d-excess) was calculated for each sample as $d\text{-excess} = \delta^2\text{H} - 8 \times \delta^{18}\text{O}$, where d-excess values less than 10 (i.e., the intercept of the Global Meteoric Water Line) indicate a sample has been partially evaporated (Dansgaard, 1964). We choose d-excess to detect evaporation because the Local Meteoric Water Line at the Konza Prairie has a similar slope and intercept as the Global Meteoric Water Line (LMWL: $\delta^2\text{H} = 7.93 \times \delta^{18}\text{O} + 10.28$, $R^2 = 0.97$; Figure S5).

2.4. Young water fractions from Bayesian Unmixing

In this study, we conducted a point-based water age estimation using a Bayesian unmixing approach to investigate both the spatial dynamics and average catchment outlet processes of water age. Bayesian unmixing was applied to the synoptic samples in the headwaters of the South Fork of Kings Creek to observe spatial dynamics of water age during stream drying, and to the NEON samples collected during the 2021 water year at the catchment outlet to observe temporal changes of water age. We used the mixing-evaporation model outlined in Bowen et al. (2018) to estimate the proportion of streamwater less than ~3 months in age at each sampling point during drying, hereafter referred to as young water fraction, F_{yw} , because it represents the same F_{yw} metric based on sinusoidal models first proposed by Kirchner (2016a) and described in detail in Section 2.5. In doing so, we assumed that the isotopic signal in streamwater reflects an integrated mix of seasonally-distinct precipitation signals, dependent on their pathways to streamflow. We defined two amount-weighted sources contributing to

streamflow: (1) precipitation that fell less than ~3 months ago and (2) precipitation older than 3 months. These age distributions were chosen to split precipitation into two isotopically-distinct sources, where the distribution for less than ~3 months in age represents the isotopic properties of spring/early summer precipitation, while the distribution for greater than ~3 months in age represents the isotopic properties of the long-term average precipitation. Groundwater was not included as a separate endmember in the unmixing analysis. Due to the non-perennial nature of our study site and unequal distribution of precipitation between spring and fall (Figure 2), we postulate that this method is well-suited for our study site although it could not be recommended for its general use.

The mixing-evaporation model (*mixSource*) is available in the *isoWater* package in R (Bowen, 2022) and uses Markov Chain Monte Carlo sampling to generate a posterior distribution of source mixtures conditioned on the observed isotopic values. In brief, the model predicts the measured isotopic composition (δ_{obs}) of a water sample from the values of an unevaporated source water (δ_s) as:

$$\delta^{18}O_{obs} = \delta^{18}O_s + E \quad (1)$$

$$\delta^2H_{obs} = \delta^2H_s + E \times m \quad (2)$$

where E is an evaporation index (in units of $\delta^{18}O$) and m is the slope of the evaporation line (EL). Prior estimates are provided for each term on the right side of the equations, and the model is inverted using Bayes Rule to obtain a posterior distribution for all model parameters conditioned on the observed sample values. Prior estimates were provided to the package for the two precipitation sources represented as bivariate normal distributions and the evaporation line represented by a normal distribution. The slope of the evaporation line ($m = 6.00 \pm 0.55$) was estimated as a linear regression fit to the stream isotopes during the summer dry-down ($R^2 = 0.99$; Figure S5). The prior describing the relative contributions of each source was left uniformed. For all analyses, three chains were generated, each run to a length of 200,000 samples with thinning to retain 7,500 samples per chain. Convergence was assessed with the R-hat statistic ($R\text{-hat} < 1.05$) and effective sample size (mean = 930), indicating good model convergence.

2.5. Young water fractions from sinusoidal models

To offer a comparison to the results obtained with the Bayesian unmixing approach and to provide insights into average young water dynamics over the 2015-2022 period with varying meteorological conditions, we estimated young water fractions using sine-wave fitting methods described in Kirchner (2016a). Kirchner (2016a and b) proposed the young water fraction, F_{yw} , as an age metric that quantifies the amount of water less than approximately 2.3 ± 0.8 months in age, and

demonstrated in modeling experiments that it could be reliably estimated for a wide range of catchment transit time distributions, including those that are heterogenous and nonstationary. The seasonal isotopic signal in precipitation and streamwater can be modeled as:

$$\delta^{18}O_P(t) = A_P * \sin(2\pi ft - \varphi_P) + k_P \quad (3)$$

$$\delta^{18}O_S(t) = A_S * \sin(2\pi ft - \varphi_S) + k_S \quad (4)$$

where $\delta^{18}O_P(t)$ and $\delta^{18}O_S(t)$ are $\delta^{18}O$ (‰) in precipitation and streamwater at time t , f is the frequency (yr^{-1} , equal to 1 for a full annual cycle), t is the time (fractional years), φ is the phase of the seasonal cycle (rad), and k is a constant describing the vertical offset of the $\delta^{18}O$ signal. $\delta^{18}O_P(t)$ was amount-weighted to give less weight to periods of low precipitation. Both time- and flow-weighted $\delta^{18}O_S(t)$ were determined to evaluate the impacts on A_S when $\delta^{18}O$ was weighted evenly compared to when more importance was given to $\delta^{18}O$ samples collected during the flowing season. The coefficients A , φ , and k were estimated using nonlinear least squares regression with a Gauss-Newton algorithm.

The F_{yw} was calculated as the amplitude ratios of $\delta^{18}O$ in precipitation and streamwater:

$$F_{yw} = A_S/A_P \quad (5)$$

Uncertainty in F_{yw} was evaluated using Gaussian error propagation where A , φ , and k were sampled 1,000 times from normal distributions with standard deviations equal to the standard errors on the fitted coefficients (Figure S7, Figure S8). The F_{yw} was then calculated 1,000 times based on the sampled parameters with uncertainty reported in terms of a standard deviation.

2.6. Discharge sensitivity of young water fractions

The discharge sensitivity of young water fractions is an analysis designed to compare the hydrological behavior of water age dynamics in different catchments with each other. Von Freyberg et al. (2018) introduced a linear equation to describe the sensitivity between increases in F_{yw} with increasing discharge (Q) and to facilitate comparison between their study catchments. Gallart et al. (2020b) developed this method further by using an exponential equation (asymptotically-constrained to the range of physically possible F_{yw} values) to describe the same relationship between F_{yw} and increasing Q , only exponentially:

$$F_{yw}(Q) = 1 - (1 - F_0) * \exp(-Q * S_d) \quad (6)$$

where F_0 is the virtual F_{yw} for $Q = 0$ and S_d (Q^{-1}) is the discharge sensitivity metric.

Gallart et al. (2020b) estimated F_0 and S_d by fitting a sinusoidal model to the seasonal $\delta^{18}O$ signal in streamwater as a function of Q :

$$\delta^{18}O_S(Q, t) = A_P * [1 - (1 - F_0) * \exp(-Q * S_d)] * \sin(2\pi ft - \varphi_S) + k_S \quad (7)$$

where $\delta^{18}O_s(Q, t)$ is the $\delta^{18}O$ (‰) in streamwater at time t and all other parameters are as defined above. The coefficients F_0 and S_d were estimated using nonlinear least squares regression with a Gauss-Newton algorithm, and their uncertainty are reported in terms of standard errors on the fitted coefficients.

We evaluated the discharge sensitivity of F_{yw} using both the Bayesian unmixing approach and sine-wave fitting methods to describe $F_{yw}(Q)$ in three experiments: (1) F_0 and S_d were estimated directly from the Bayesian-unmixed F_{yw} values using Eq. 6 for the 2021 water year, (2) F_0 and S_d were estimated using Eq. 7 for the 2021 water year, and (3) F_0 and S_d were estimated using Eq. 7 for the long-term record of $\delta^{18}O$ samples at the NEON sampling site. In experiment 2 and 3, F_0 and S_d values obtained from sine-wave fitting were then used in Eq. 7 to model $F_{yw}(Q)$.

3. Results & Discussion

3.1. Spatiotemporal Patterns in Stream $\delta^{18}\text{O}$ Compositions

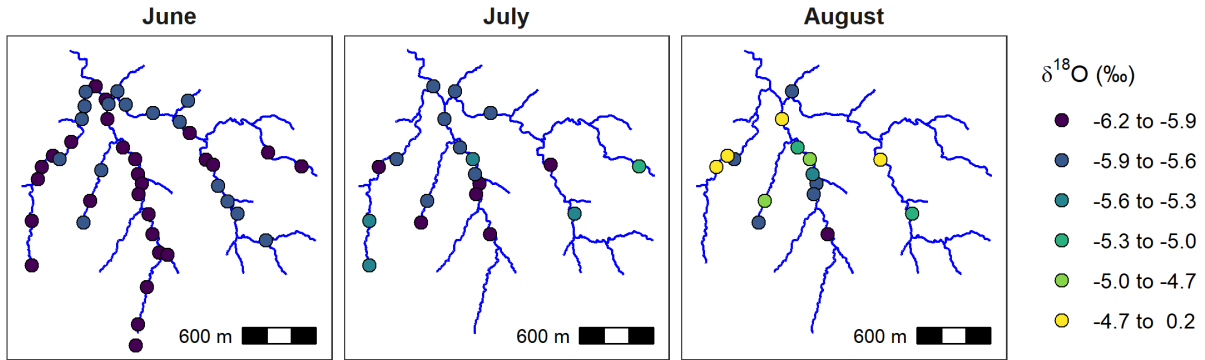


Figure 3. Spatial variation in $\delta^{18}\text{O}$ during the summer dry-down period.

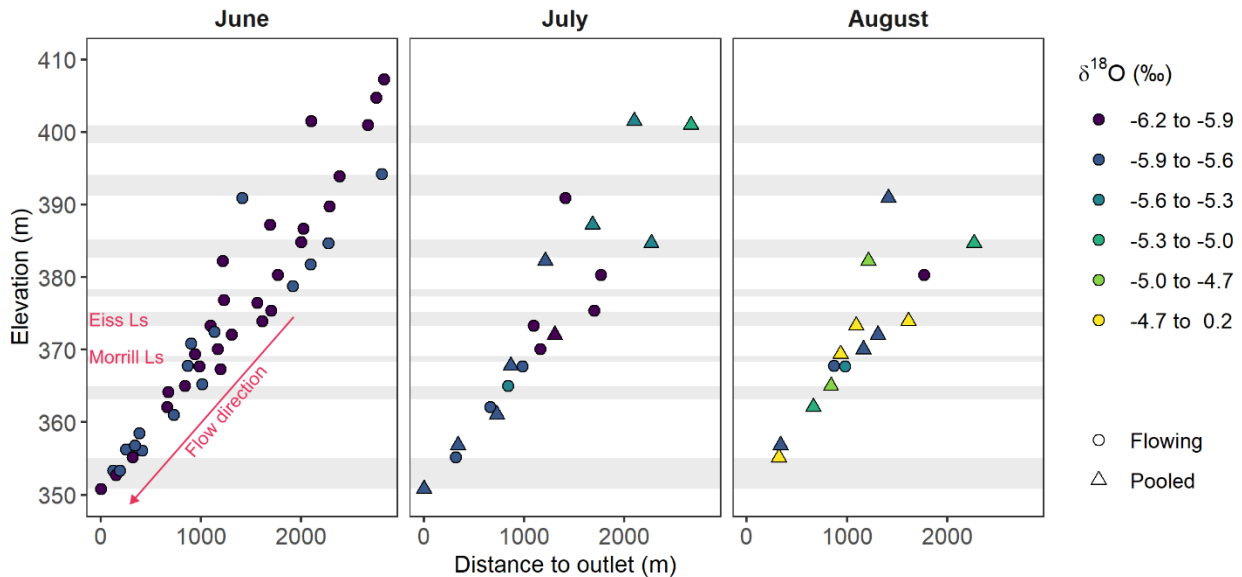


Figure 4. Variation in $\delta^{18}\text{O}$ with distance to outlet during the summer dry-down period. Samples were categorized as flowing (circles) or pooled (triangles) at the time of collection. Approximate elevations where limestone units outcrop the watershed are shown as gray bands (mapped in Figure S3). These elevations are based on average member thickness in the drilling log records at the Konza Prairie.

Over June, July, and August 2021, the South Fork of Kings Creek shifted from a fully flowing, connected system to a network of isolated pools concentrated in mid-elevations (Figure 3, Figure 4). The stream network went from 86% wet in June, to 38% wet in July, to 30% wet in August (Figure 3). Stream network wetness was determined as the proportion of sampling sites with water present (either flowing

or pooled) compared to the total number of sampling sites visited. Stream drying occurred between June and August at elevations below ~355 m and above ~390 m, while mid-elevations in the watershed remained wet (Figure 4). Stream drying fragmented the network into a series of flowing reaches and isolated pools, with pools representing most of the surface water in August (Figure 4). Based on past studies that have linked flow to storage thresholds in the underlying limestone aquifers (Costigan et al., 2015; Hatley et al., 2022). We interpret this widespread wet to dry transition as a reversal of stream-aquifer gradient, whereby the stream transitioned from a net gaining condition (flow from groundwater into the stream) to a net losing condition (flow from the stream into the groundwater system) during the summer. However, we interpret groundwater-surface water interactions as spatially variable, and localized points of drying are likely where the stream infiltrated and recharged the aquifer at that location and/or upstream, while points where flow is sustained throughout the summer are likely at or immediately downstream of persistent groundwater discharge points.

Surface water persisted at elevations in the range of several limestone aquifers, including the Eiss and Morill aquifers (Figure 4). Thin 1 – 2 m karstified limestone formations throughout the catchment are thought to be the primary source of water sustaining flow in the South Fork of Kings Creek based on end-member mixing analysis (Hatley et al., 2022; Keen et al., 2022; Sullivan et al., 2019). In the same catchments, Hatley et al. (2022) found groundwater discharge contributed > 95% of streamflow during their sampling events, which spanned from April through July (2021), with minimal streamflow sourced from soil water (< 1%) and direct surface runoff (< 4%). Konza's alternating karstified limestone formations sustain surface water presence where they outcrop at mid-elevations in the watershed during the driest parts of the year, typically late summer. Groundwater is known to sustain flow in a range of systems from small headwater non-perennial streams (Hatley et al., 2022; Warix et al., 2021) to large intermittent rivers (Zipper et al., 2022; Vu et al., 2018). In instances where human alterations to the water cycle, e.g., groundwater pumping or surface water diversions, are unimportant, such as Kings Creek, it is local groundwater and its bidirectional flow to the stream that controls flow permanence and produces nuanced wetting and drying patterns in space and time (Zimmer and McGlynn, 2017).

The $\delta^{18}\text{O}$ composition of streamwater was progressively enriched during the network dry-down and variability in $\delta^{18}\text{O}$ increased considerably over the summer months (Figure 3). Stream $\delta^{18}\text{O}$ ratios in the headwaters varied in space and time, ranging from -6.0‰ to -5.8‰ in June, -6.1‰ to -5.1‰ in July, and -5.9‰ to 0.21‰ in August (Figure 3). We infer the stream to be well connected and gaining groundwater from the limestone aquifers through most of the network in June, when stream $\delta^{18}\text{O}$

compositions are similar across the network and the stream was flowing at all sampling points. However, as the limestone aquifers drained out in the dry summer weather and stream-aquifer gradients reversed, disparate portions of the watershed in space and time were disconnected from groundwater inputs, and the $\delta^{18}\text{O}$ signal in the remaining isolated pools became enriched due to evaporative effects.

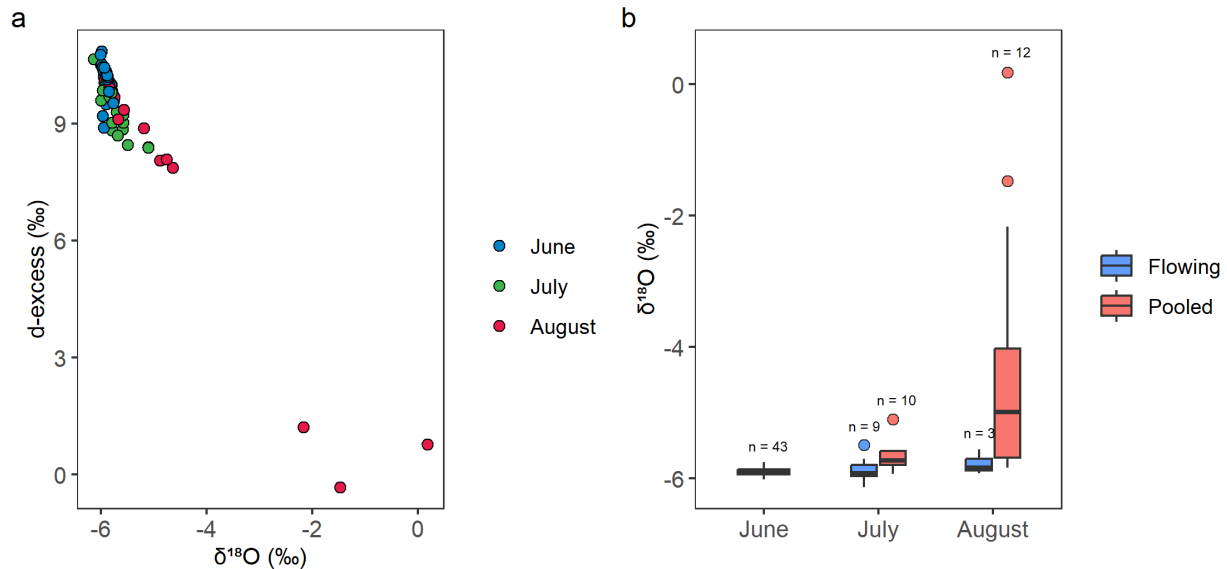


Figure 5. Variability in (a) $\delta^{18}\text{O}$ and d-excess and (b) $\delta^{18}\text{O}$ and surface water connectivity during the summer dry-down period.

We identified two interrelated factors that influence the variation in water isotopic signatures: (1) evaporative effects, as indicated by deuterium excess (d-excess; Figure 5a) and (2) a decrease in surface water connectivity (Figure 5b). Deuterium excess (d-excess) ranged from 8.9‰ to 10.9‰ in June, 8.4‰ to 10.7‰ in July, and -0.3‰ to 10.1‰ in August (Figure 5a). Shifts to lower d-excess values are consistent with removal of light water vapor from the stream water during evaporation. Thus, the degree of evaporation-induced isotopic fractionation increased throughout the summer as conditions warmed and precipitation events became less frequent. These evaporative effects also produced differences in the $\delta^{18}\text{O}$ compositions of flowing reaches compared to isolated pools by the end of the summer (Figure 5b). Further, variability in $\delta^{18}\text{O}$ ratios increased as surface water connectivity decreased and stream-aquifer directions reversed towards losing water to the underlying limestone aquifers and/or evaporated in isolated pools above impermeable mudstones. In a random forest model to predict stream $\delta^{18}\text{O}$ during the summer months, day of year and flowing/pooled reaches were the best

overall predictor for explaining observed stream $\delta^{18}\text{O}$ compositions (Figure S6), highlighting the role of disconnection in driving stream water isotopic variation.

3.2. Ages and Inferred Sources of Water Sustaining Streamflow

3.2.1. Spatiotemporal variability during dry-down

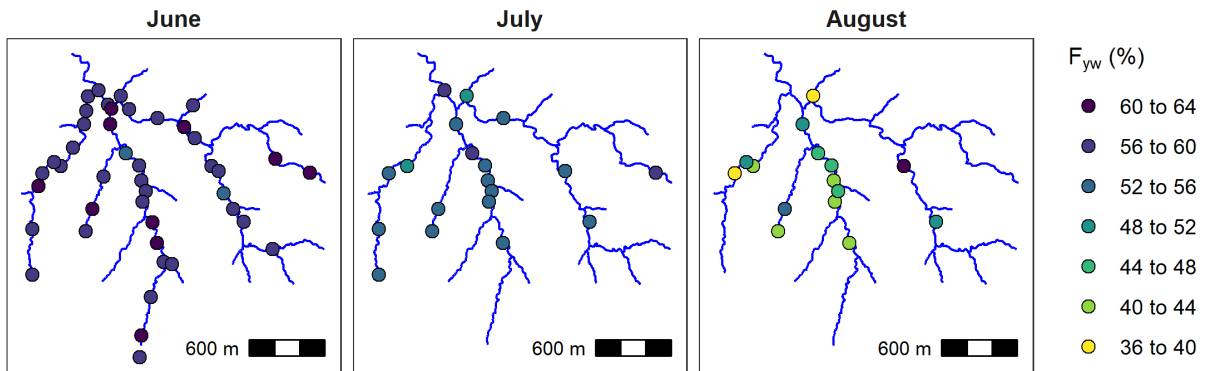


Figure 6. Young water fractions, F_{yw} , estimated from Bayesian unmixing approach. Streamflow age is defined as the mean of the posterior distribution of source mixtures.

The age of streamflow generally became older and more spatially variable over the course of the summer (Figure 6). F_{yw} estimated using the Bayesian unmixing approach ranged from 53.9% to 62.6% (mean = 58.8%) during June, when the stream network was fully connected and flowing. However, as the stream became disconnected, the proportion of young streamflow decreased and ranged from 49.5% to 59.0% (mean = 54.0%) in July and 39.1% to 62.0% (mean = 46.4%) in August (Figure 6). We interpret these results, which account for the effects of evaporation constrained by the local evaporation line and its uncertainty, to reflect a shift in groundwater inputs to the stream, from fast-draining flowpaths in June to more slowly draining flowpaths from lower permeability horizons later in the summer. There is minimal variation in water age in June, when most of the stream network received young water from recent precipitation and flow throughout the network homogenized estimated water age.

However, as the aquifers drained out in the dry summer weather, older water sustained flows with increased variability in water age as the stream network transitioned from wet to dry and stream-aquifer directions reversed so that the stream was primarily losing water to the groundwater system. In July and August, the percentage of older water increased, presumably from water with more varied age compositions being transported through less permeable pore space and reduced mixing due to decreased surface water connectivity (Figure 4), though network-wide approximately half of the stream

water was still young water. The high F_{yw} estimates align with past studies that have shown preferential flow (i.e., soil macropores, fractures, solution-enlarged pores, and springs) to be important in this watershed, as these flowpaths can quickly route water to the stream (Macpherson and Sullivan, 2019; Tsy-pin and Macpherson, 2012; Macpherson et al., 2008). Similarly high young water fractions (reaching up to 40%) and short mean transit times (0.34 to 0.74 years) have been reported in other small headwater non-perennial streams in karst aquifers, where young water is likely transmitted via well-developed karst conduits (Rusjan et al., 2019).

3.2.2. Implications at watershed outlet

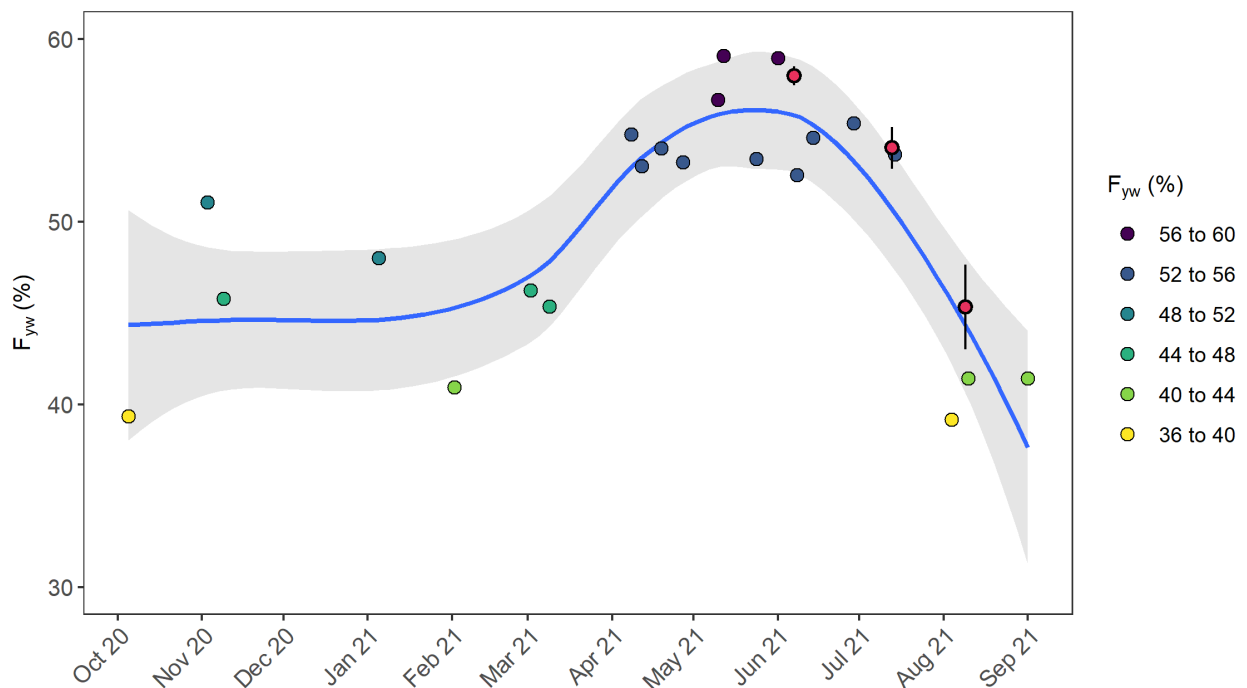


Figure 7. Young water fractions, F_{yw} , estimated from Bayesian unmixing at the NEON sampling site. For comparison, the red dots show the average and 95% confidence interval of all the synoptic sampling points (i.e., all points in Figure 6). The blue line and shaded interval show a loess fit with its 95% confidence interval for the Bayesian unmixing of the NEON sampling site.

Streamflow at the catchment outlet was younger when the network was fully-connected and flowing, and became older and temporally variable as the network transitioned to a state of drying (Figure 7). F_{yw} estimated using the Bayesian unmixing approach ranged from 39.2% to 59.1% in 2021, with older water contributions the greatest during the driest parts of the year in late summer, fall, and winter. The age of streamflow at the catchment outlet followed the same trajectory as in the

headwaters, and thus we observed good agreement in water age estimates between the Bayesian unmixing of the synoptic samples and the downstream NEON samples. Additionally, we used sinusoidal methods to estimate average young water fractions for 2015 to 2022 to provide a comparison to the Bayesian model results. We found that multi-year average F_{yw} values obtained using sinusoidal models were smaller than those of the Bayesian model with a flow-weighted F_{yw} of $15.29\% \pm 5.73$ and a time-weighted F_{yw} of $4.05\% \pm 2.00$.

There are several potential explanations for the differences in F_{yw} estimates between the sinusoidal and Bayesian approaches. First, the two methods were applied over different time periods, with the sinusoidal approach providing an average F_{yw} estimate for the 2015-2022 period while the Bayesian method was only used in 2021. Different hydrometeorological conditions during these periods may have led to differences in water storage and discharge dynamics within the catchment, as the catchments are currently undergoing a long-term drying trend (Sadayappan et al., 2023). Alternatively, the two modeling approaches may disagree due to challenges associated with fitting each of the separate models. For example, due to the seasonal cycle of isotopic compositions (i.e., Figure S8), the Bayesian unmixing approach may be inadvertently identifying some spring rainfalls from previous years as young water in 2021. Uncertainty in sinusoidal model fitting may result from evaporated streamwater samples during late summer and fall and from flow-weighting, since discharge is particularly challenging to measure accurately when streams approach dry conditions (Seybold et al., 2023). However, even if these challenges lead to disagreement in the precise value of F_{yw} between methods, the combined spatial and temporal evolution of water age still suggests a shift away from rapid fracture flow towards slower matrix flow that creates a sustained but localized surface water presence during the driest parts of the year that is mirrored in both the headwaters and at the outlet.

3.3 Sensitivity of young water fractions to hydrological conditions

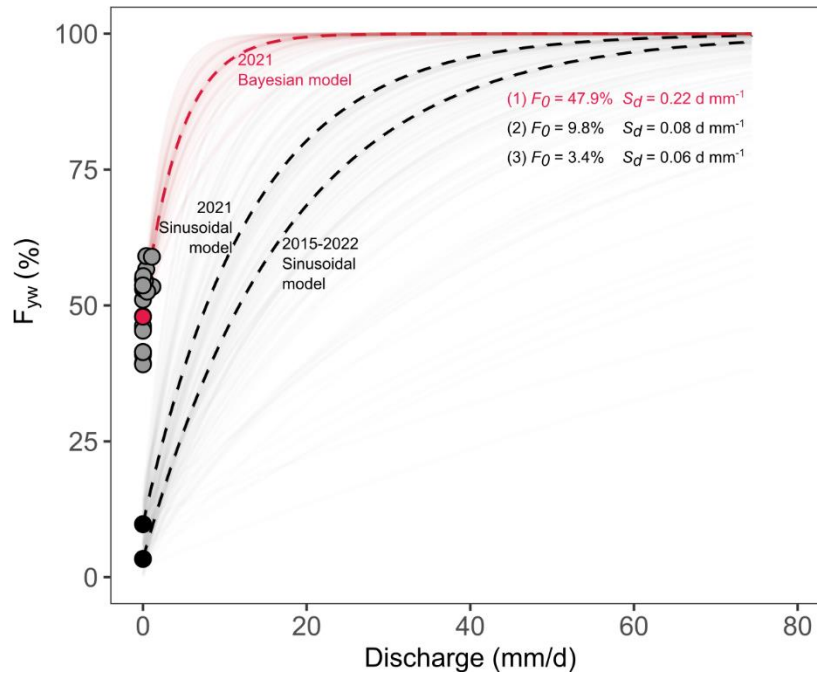


Figure 8. Sensitivity of young water fractions, F_{yw} , to discharge obtained from the Bayesian model and sine-wave fitting methods. The curves represent exponential fits of the $F_{yw}(Q)$ model (Eq. 6) proposed by Gallart et al. (2020b) for three experiments: (1) Bayesian-estimated discharge sensitivity during the 2021 water year, (2) sinusoidal-based discharge sensitivity during the 2021 water year, and (3) sinusoidal-based discharge sensitivity for years spanning 2015 to 2022 with variable hydrometeorological conditions. The black and red points are the estimated F_0 parameters for each method. The grey points are the Bayesian-estimated young water fractions (points shown in Figure 7).

Our modeling experiments showed young water fractions to be highly sensitive to hydrometeorological conditions in Kings Creek regardless of the method used, though the fitted parameters, F_0 and S_d , differed between the Bayesian model and sine-wave fitting methods (Figure 8). The Bayesian model yielded a higher F_{yw} for $Q = 0$, F_0 , of $47.9\% \pm 1.4$ and a higher discharge sensitivity, S_d , of $0.22 \text{ dmm}^{-1} \pm 0.08$ compared to sine-wave fitting method with $F_0 = 9.8\% \pm 2.9$ and $S_d = 0.08 \text{ dmm}^{-1} \pm 0.06$ during the 2021 water year. For the years spanning 2015 to 2022 with different hydrometeorological conditions, $F_0 = 3.4\% \pm 2.2$, while the discharge sensitivity was similar, but slightly less than in a wetter year on record, $S_d = 0.06 \text{ dmm}^{-1} \pm 0.03$. The observed discharge sensitivity of Kings Creek is on the higher end of S_d values reported for other catchments (Von Freyberg et al. 2018; Gallart et al. 2020a), which is consistent with past work showing that its flashy, non-perennial flow regime and

complex merokarst geology can lead to a rapid hydrologic response to precipitation through discharge of groundwater (Hatley et al., 2023).

3.4 Synthesizing evidence of water age and source in non-perennial streams

Multiple studies have concluded that groundwater sustains flow in the South Fork of Kings Creek (Hatley et al., 2022; Keen et al., 2022; Sullivan et al., 2019); however, the transit time for groundwater to reach the stream remained unknown. We found the South Fork of Kings Creek shifted from a fully flowing, connected system to a network of isolated pools, where surface water persisted due to groundwater inputs from the many limestone aquifers (Figure 3 and 4). During the network dry-down, the $\delta^{18}\text{O}$ composition of streamwater was progressively enriched due to evaporative effects and a decrease in surface water connectivity (Figure 5). Multiple lines of evidence suggest that a substantial amount of summer streamflow (up to 62.6% at points based on the Bayesian unmixing approach) originated as young water sourced from spring rains and high-intensity summer storms (Figure 6 and 7), and that young water releases from catchment storage are highly sensitive to hydrometeorological conditions (Figure 8)

Streamflow in the South Fork of Kings Creek and at the outlet is a mixture of young and old water, with increasing age as the stream network dries, indicating that old water can be stored in the subsurface but remain disconnected from the stream for part of the year. Understanding this mixture of young and old water in generating streamflow provides another line of evidence for the “fill and spill” hydrology hypothesized to operate in the Konza Prairie and other similar merokarst settings, where storage thresholds control flow permanence (Costigan et al., 2015; McDonnell et al., 2021). In brief, when the watershed is dry, precipitation infiltrates into the subsurface to “fill” the many limestone aquifers, but does not push groundwater to the stream. However, as the limestone aquifers exceed some critical threshold of storage, they “spill” by pushing groundwater to the stream. At the point when storage thresholds are exceeded, precipitation and streamflow patterns are synchronized, meaning that discharge tends to increase contemporaneously with precipitation events, ultimately recoupling the hydrologic flow regime of the stream to sub-annual weather patterns (Costigan et al., 2015).

For instance, in 2021 we observed the onset of fill to end of spill, where it rained above average in March (81.5 percentile of 30 year conditions), but this precipitation did not generate streamflow until the limestone aquifers had “filled” by the start of April, representing a period of time when precipitation and streamflow patterns were desynchronized (Figure 2). Our results suggest that spring and early summer rains provided a substantial flux of young water that was transmitted to the underlying

limestone aquifers through soil macropores and bedrock fractures (noted in Macpherson and Sullivan, 2019; Tsy-pin and Macpherson, 2012; Macpherson et al., 2008) and, once storage thresholds were exceeded, the stream network transitioned to flowing and connected, recoupling the response of streamflow to precipitation. As the stream dried, the shift in water age indicates a shift in water sources from within-year preferential groundwater discharge to much older groundwater that was pushed out of less permeable matrix pore space. In addition to the within-year shifts to deeper, slower flowpaths as the network dries, which are suggested by our work, recent studies have also indicated that long-term woody vegetation encroachment within these catchments is promoting shifts to deeper flowpaths and drier conditions over decadal timescales (Sadayappan et al., 2023). Taken together, these findings indicate that seasonal contributions of young water drive storage above critical thresholds causing wet-up, while old water is more slowly pushed out of the less permeable pore space thereby sustaining surface water during the driest parts of summer, and that the relative partitioning of these different flowpaths is threatened by woody vegetation encroachment.

3.5 Implications for water management and policy

Non-perennial streams are the source of considerable policy and management debate; in the US, much of the debate centers on their connection to downstream sources (see Section 1). Thus, our demonstration of the prevalence of relatively fast flowpaths in sustaining flow in non-perennial streams provides a structural “significant nexus” between activities on the landscape, non-perennial headwater streams, and their downstream perennial rivers in merokarst regions. Therefore, our results suggest that management decisions that impair water quality and/or quantity in non-perennial watersheds have the potential to “significantly affect the chemical, physical, and biological integrity” of downstream navigable waters (Clean Water Rule, 2015). Due to the predominance of fast flowpaths sustaining streamflow in Kings Creek, nutrients and contaminants have the potential to be transported over short timescales from the landscape to the stream, with little time for attenuation.

These fast flowpaths may exert a disproportionate influence on downstream water quality. For example, in agricultural regions, nitrate from farming operations has extensively degraded surface and groundwater quality; the prevalence of fast groundwater flowpaths in regions with high legacy nitrogen load could contribute to on-going declines in surface water quality (Byrnes et al., 2020; Van Meter et al., 2018; Van Meter et al., 2016). As another example, even much longer groundwater flowpaths have been shown to transport contaminants over sub-annual timescales (< 10 months), as seen in the contentious County of Maui, Hawaii v. Hawaii Wildlife Fund case (Cornwall, 2020; Craig et al., 2013). Degradation of

water quality could be further compounded by changes in water availability driven by short-term hydroclimatic change and longer-term changes in groundwater dynamics, which could cause downstream perennial waters to receive increasingly variable streamflows, with potential to affect our ability to meet both agricultural and domestic water requirements. These climate-driven changes may be compounded by modifications to land use, such as urbanization that can alter partitioning of water between runoff and groundwater recharge (Zipper et al., 2017), deforestation for agricultural expansion that can increase groundwater levels (Gimenez et al., 2016), or woody vegetation encroachment which can decrease recharge and streamflow in grasslands (Keen et al., 2022; Sadayappan et al., 2023). Indeed, given the potential for climate and land use-driven changes to hydrology, policymakers and water managers may need to account for the potential fast transit of water from the landscape to non-perennial streams to downstream perennial waters.

4. Conclusions

We used water isotopes with a Bayesian unmixing approach to estimate young water fractions, water source, and associated changes in a non-perennial stream network at the Konza Prairie during the 2021 summer dry-down season, as well as over a multi-year period with varying hydrometeorological conditions. We found pronounced spatial and temporal variability in stream $\delta^{18}\text{O}$ compositions during the summer dry-down period due to evaporative effects and a decrease in surface water connectivity. Using a Bayesian model, we found that a substantial amount of streamflow in the South Fork of Kings Creek originated as young water sourced from within-season precipitation that had been stored in the subsurface for less than ~ 3 months, regardless of position in the watershed, during the 2021 water year, and that spatial variability in young water fractions increased as the network dried. Over multiple years, we found that young water contributions estimated using sinusoidal models were smaller than Bayesian estimates, but both modeling approaches suggest young water fractions are highly sensitive to hydrological conditions, with streamwater shifting to older sources as drying progressed. We interpret this water age transition as a shift in water source towards less permeable and slower subsurface flowpaths that sustain flow during the driest parts of the year. The predominance of young water routed along fast flowpaths suggests a rapid connection between these upstream headwaters to downstream perennial waters, indicating that changes to water quality and/or quantity in non-perennial streams have the potential to cause significant downstream consequences.

Acknowledgments

We thank all collaborators on Aquatic Intermittency Effects of Microbiomes in Streams (AIMS) who assisted in the synoptic sampling campaigns, as well as the Konza Prairie Biological Station and its staff for site access and management. Specifically, we thank Sarah Flynn, Simmi Rana, Jessica Wilhelm, Michelle Wolford and Kaci Zarek for the additional sample collection field work in July and August. Additionally, we would like to thank the National Ecological Observatory Network and the Konza Prairie Long Term Ecological Research programs for their long-term data collection efforts which supported our analysis, and conversations with Gwen MacPherson and Walter Dodds on the hydrology of Konza. This manuscript was also improved by constructive feedback from Drs. Simone Fatichi, Francesc Gallart, and two anonymous reviewers. Support was provided by a National Science Foundation awards OIA-2019603 and DEB-2025849.

Open Research

The data and scripts associated with this study are available in the Zenodo repository at:

<https://doi.org/10.5281/zenodo.7633403>

References

- Alexander, L. C. (2015). Science at the boundaries: scientific support for the Clean Water Rule. *Freshwater Science*, 34(4), 1588–1594. <https://doi.org/10.1086/684076>
- Allen, D. C., Datry, T., Boersma, K. S., Bogan, M. T., Boulton, A. J., Bruno, D., et al. (2020). River ecosystem conceptual models and non-perennial rivers: A critical review. *WIREs Water*, 7(5), e1473. <https://doi.org/10.1002/wat2.1473>
- Barry, E. (2018). Characterizing groundwater flow through merokarst, northeast, Kansas, USA (MS thesis). University of Kansas.
- Botter, G., & Durighetto, N. (2020). The Stream Length Duration Curve: A Tool for Characterizing the Time Variability of the Flowing Stream Length. *Water Resources Research*, 56(8), e2020WR027282. <https://doi.org/10.1029/2020WR027282>
- Bowen, G. J. (2022). isoWater: Discovery, retrieval, and analysis of water isotope data (Version 1.1.1). Retrieved from <https://CRAN.R-project.org/package=isoWater>
- Bowen, G. J., Putman, A., Brooks, J. R., Bowling, D. R., Oerter, E. J., & Good, S. P. (2018). Inferring the source of evaporated waters using stable H and O isotopes. *Oecologia*, 187(4), 1025–1039. <https://doi.org/10.1007/s00442-018-4192-5>

- Brookfield, A. e., Macpherson, G. I., & Covington, M. d. (2017). Effects of Changing Meteoric Precipitation Patterns on Groundwater Temperature in Karst Environments. *Groundwater*, 55(2), 227–236. <https://doi.org/10.1111/gwat.12456>
- Busch, M. H., Costigan, K. H., Fritz, K. M., Datry, T., Krabbenhoft, C. A., Hammond, J. C., et al. (2020). What's in a Name? Patterns, Trends, and Suggestions for Defining Non-Perennial Rivers and Streams. *Water*, 12(7), 1980. <https://doi.org/10.3390/w12071980>
- Byrnes, D. K., Van Meter, K. J., & Basu, N. B. (2020). Long-Term Shifts in U.S. Nitrogen Sources and Sinks Revealed by the New TREND-Nitrogen Data Set (1930–2017). *Global Biogeochemical Cycles*, 34(9), e2020GB006626. <https://doi.org/10.1029/2020GB006626>
- Clean Water Rule: Definition of “Waters of the United States.” (2015, June 29). Retrieved from <https://www.federalregister.gov/documents/2015/06/29/2015-13435/clean-water-rule-definition-of-waters-of-the-united-states>
- Cornwall, W. (2020, April 23). ‘Hydrologists should be happy.’ Big Supreme Court ruling bolsters groundwater science. *Science*. Retrieved from <https://www.science.org/content/article/scotus-clean-water>
- Costigan, K. H., Daniels, M. D., & Dodds, W. K. (2015). Fundamental spatial and temporal disconnections in the hydrology of an intermittent prairie headwater network. *Journal of Hydrology*, 522, 305–316. <https://doi.org/10.1016/j.jhydrol.2014.12.031>
- Craig, H. (1961). Isotopic Variations in Meteoric Waters. *Science*, 133(3465), 1702–1703. <https://doi.org/10.1126/science.133.3465.1702>
- Dansgaard, W. (1964). Stable isotopes in precipitation. *Tellus*, 16(4), 436–468. <https://doi.org/10.1111/j.2153-3490.1964.tb00181.x>
- Datry, T., Truchy, A., Olden, J. D., Busch, M. H., Stubbington, R., Dodds, W. K., et al. (2023). Causes, Responses, and Implications of Anthropogenic versus Natural Flow Intermittence in River Networks. *BioScience*, 73(1), 9–22. <https://doi.org/10.1093/biosci/biac098>
- DelVecchia, A. G., Shanafield, M., Zimmer, M. A., Busch, M. H., Krabbenhoft, C. A., Stubbington, R., et al. (2022). Reconceptualizing the hyporheic zone for nonperennial rivers and streams. *Freshwater Science*, 41(2), 167–182. <https://doi.org/10.1086/720071>
- von Freyberg, J., Allen, S. T., Seeger, S., Weiler, M., & Kirchner, J. W. (2018). Sensitivity of young water fractions to hydro-climatic forcing and landscape properties across 22 Swiss catchments. *Hydrology and Earth System Sciences*, 22(7), 3841–3861. <https://doi.org/10.5194/hess-22-3841-2018>

- Gallart, F., Valiente, M., Llorens, P., Cayuela, C., Sprenger, M., & Latron, J. (2020a). Investigating young water fractions in a small Mediterranean mountain catchment: Both precipitation forcing and sampling frequency matter. *Hydrological Processes*, 34(17), 3618–3634. <https://doi.org/10.1002/hyp.13806>
- Gallart, F., von Freyberg, J., Valiente, M., Kirchner, J. W., Llorens, P., & Latron, J. (2020b). Technical note: An improved discharge sensitivity metric for young water fractions. *Hydrology and Earth System Sciences*, 24(3), 1101–1107. <https://doi.org/10.5194/hess-24-1101-2020>
- Giménez, R., Mercau, J., Nosetto, M., Páez, R., & Jobbágy, E. (2016). The ecohydrological imprint of deforestation in the semiarid Chaco: insights from the last forest remnants of a highly cultivated landscape. *Hydrological Processes*, 30(15), 2603–2616. <https://doi.org/10.1002/hyp.10901>
- Glenn, C. R., Whittier, R. B., Dailer, M. L., Dulaiova, H., El-Kadi, A. I., Fackrell, J., et al. (2013). Lahaina groundwater tracer study -- Lahaina, Maui, Hawaii. Retrieved from <http://hdl.handle.net/10125/50768>
- Gómez, R., Arce, M. I., Baldwin, D. S., & Dahm, C. N. (2017). Chapter 3.1 - Water Physicochemistry in Intermittent Rivers and Ephemeral Streams. In T. Datry, N. Bonada, & A. Boulton (Eds.), *Intermittent Rivers and Ephemeral Streams* (pp. 109–134). Academic Press. <https://doi.org/10.1016/B978-0-12-803835-2.00005-X>
- Hale, R. L., & Godsey, S. E. (2019). Dynamic stream network intermittence explains emergent dissolved organic carbon chemostasis in headwaters. *Hydrological Processes*, 33(13), 1926–1936. <https://doi.org/10.1002/hyp.13455>
- Hammond, J. C., Zimmer, M., Shanafield, M., Kaiser, K., Godsey, S. E., Mims, M. C., et al. (2021). Spatial Patterns and Drivers of Nonperennial Flow Regimes in the Contiguous United States. *Geophysical Research Letters*, 48(2), e2020GL090794. <https://doi.org/10.1029/2020GL090794>
- Hatley, C. M., Armijo, B., Andrews, K., Anhold, C., Nippert, J. B., & Kirk, M. F. (2023). Intermittent streamflow generation in a merokarst headwater catchment. *Environmental Science: Advances*, 2(1), 115–131. <https://doi.org/10.1039/D2VA00191H>
- Hayden, B. P. (n.d.). Regional climate and the distribution of tallgrass prairie. In A. K. Knapp, J. M. Briggs, D. C. Hartnett, & S. L. Collins (Eds.), *Grassland Dynamics* (pp. 19–34). New York: Oxford University Press.

- Hrachowitz, M., Benettin, P., van Breukelen, B. M., Fovet, O., Howden, N. J. K., Ruiz, L., et al. (2016). Transit times—the link between hydrology and water quality at the catchment scale. *WIREs Water*, 3(5), 629–657. <https://doi.org/10.1002/wat2.1155>
- Jasechko, S. (2019). Global Isotope Hydrogeology—Review. *Reviews of Geophysics*, 57(3), 835–965. <https://doi.org/10.1029/2018RG000627>
- Jensen, C. K., McGuire, K. J., McLaughlin, D. L., & Scott, D. T. (2019). Quantifying spatiotemporal variation in headwater stream length using flow intermittency sensors. *Environmental Monitoring and Assessment*, 191(4), 226. <https://doi.org/10.1007/s10661-019-7373-8>
- Keen, R. M., Nippert, J. B., Sullivan, P. L., Ratajczak, Z., Ritchey, B., O’Keefe, K., & Dodds, W. K. (2022). Impacts of Riparian and Non-riparian Woody Encroachment on Tallgrass Prairie Ecohydrology. *Ecosystems*. <https://doi.org/10.1007/s10021-022-00756-7>
- Kirchner, J. W. (2016a). Aggregation in environmental systems Part 1: Seasonal tracer cycles quantify young water fractions, but not mean transit times, in spatially heterogeneous catchments. *Hydrology and Earth System Sciences*, 20(1), 279–297. <https://doi.org/10.5194/hess-20-279-2016>
- Kirchner, J. W. (2016b). Aggregation in environmental systems Part 2: Catchment mean transit times and young water fractions under hydrologic nonstationarity. *Hydrology and Earth System Sciences*, 20(1), 299–328. <https://doi.org/10.5194/hess-20-299-2016>
- Krabbenhoft, C. A., Allen, G. H., Lin, P., Godsey, S. E., Allen, D. C., Burrows, R. M., et al. (2022). Assessing placement bias of the global river gauge network. *Nature Sustainability*, 5(7), 586–592. <https://doi.org/10.1038/s41893-022-00873-0>
- Lapides, D. A., Hahm, W. J., Rempe, D. M., Dietrich, W. E., & Dralle, D. N. (2022). Controls on Stream Water Age in a Saturation Overland Flow-Dominated Catchment. *Water Resources Research*, 58(4), e2021WR031665. <https://doi.org/10.1029/2021WR031665>
- Leone, M., Gentile, F., Lo Porto, A., Ricci, G. F., & De Girolamo, A. M. (2023). Ecological flow in southern Europe: Status and trends in non-perennial rivers. *Journal of Environmental Management*, 342, 118097. <https://doi.org/10.1016/j.jenvman.2023.118097>
- Liptak, A. (2023, May 25). Supreme Court Limits E.P.A.’s Power to Address Water Pollution. *The New York Times*. Retrieved from <https://www.nytimes.com/2023/05/25/us/supreme-court-epa-water-pollution.html>

- Logan, K. E., & Brunzell, N. A. (2015). Influence of drought on growing season carbon and water cycling with changing land cover. *Agricultural and Forest Meteorology*, 213, 217–225.
<https://doi.org/10.1016/j.agrformet.2015.07.002>
- Macpherson, G. L. (1996). Hydrogeology of thin limestones: the Konza Prairie Long-Term Ecological Research Site, Northeastern Kansas. *Journal of Hydrology*, 186(1), 191–228.
[https://doi.org/10.1016/S0022-1694\(96\)03029-6](https://doi.org/10.1016/S0022-1694(96)03029-6)
- Macpherson, G. L., & Sullivan, P. L. (2019). Watershed-scale chemical weathering in a merokarst terrain, northeastern Kansas, USA. *Chemical Geology*, 527, 118988.
<https://doi.org/10.1016/j.chemgeo.2018.12.001>
- Macpherson, G. L., Roberts, J. A., Blair, J. M., Townsend, M. A., Fowle, D. A., & Beisner, K. R. (2008). Increasing shallow groundwater CO₂ and limestone weathering, Konza Prairie, USA. *Geochimica et Cosmochimica Acta*, 72(23), 5581–5599.
<https://doi.org/10.1016/j.gca.2008.09.004>
- Maher, K. (2010). The dependence of chemical weathering rates on fluid residence time. *Earth and Planetary Science Letters*, 294(1), 101–110. <https://doi.org/10.1016/j.epsl.2010.03.010>
- McDonnell, J. J., Spence, C., Karran, D. J., van Meerveld, H. J. (Ilja), & Harman, C. J. (2021). Fill-and-Spill: A Process Description of Runoff Generation at the Scale of the Beholder. *Water Resources Research*, 57(5), e2020WR027514. <https://doi.org/10.1029/2020WR027514>
- Messenger, M. L., Lehner, B., Cockburn, C., Lamouroux, N., Pella, H., Snelder, T., et al. (2021). Global prevalence of non-perennial rivers and streams. *Nature*, 594(7863), 391–397.
<https://doi.org/10.1038/s41586-021-03565-5>
- Meter, K. J. V., Basu, N. B., Veenstra, J. J., & Burras, C. L. (2016). The nitrogen legacy: emerging evidence of nitrogen accumulation in anthropogenic landscapes. *Environmental Research Letters*, 11(3), 035014. <https://doi.org/10.1088/1748-9326/11/3/035014>
- National Ecological Observatory Network (NEON). (2022a). Stable isotopes in precipitation (DP1.00038.001). National Ecological Observatory Network (NEON).
<https://doi.org/10.48443/E3MY-7V57>
- National Ecological Observatory Network (NEON). (2022b). Stable isotopes in surface water (DP1.20206.001). National Ecological Observatory Network (NEON).
<https://doi.org/10.48443/YZ7H-F560>

- Nippert, J. (2022). AWEOL Meteorological data from the Konza prairie headquarters weather station. Environmental Data Initiative. Retrieved from <http://dx.doi.org/10.6073/pasta/98b9d0a612c17ab9f8f121d9741e72a6>
- Pomes, M. (1995). A study of the aquatic humic substances and hydrogeology in a prairie watershed: Use of humic material as a tracer of recharge through soils (PhD thesis). University of Kansas.
- Price, A. N., Jones, C. N., Hammond, J. C., Zimmer, M. A., & Zipper, S. C. (2021). The Drying Regimes of Non-Perennial Rivers and Streams. *Geophysical Research Letters*, 48(14), e2021GL093298. <https://doi.org/10.1029/2021GL093298>
- Ransom, M. D., Rice, C. W., & Todd, T. C. (n.d.). Soils and soil biota. In A. K. Knapp, J. M. Briggs, D. C. Hartnett, & S. L. Collins (Eds.), *Grassland Dynamics: Long-term ecological research in tallgrass prairie* (pp. 48–66). New York: Oxford University Press.
- Revised Definition of “Waters of the United States.” (2023, January 18). Retrieved from <https://www.federalregister.gov/documents/2023/01/18/2022-28595/revised-definition-of-waters-of-the-united-states>
- Rusjan, S., Sapač, K., Petrič, M., Lojen, S., & Bezak, N. (2019). Identifying the hydrological behavior of a complex karst system using stable isotopes. *Journal of Hydrology*, 577, 123956. <https://doi.org/10.1016/j.jhydrol.2019.123956>
- Sadayappan, K., Keen, R., Jarecke, K. M., Moreno, V., Nippert, J. B., Kirk, M. F., et al. (2023). Drier streams despite a wetter climate in woody-encroached grasslands. *Journal of Hydrology*, 627, 130388. <https://doi.org/10.1016/j.jhydrol.2023.130388>
- Sauquet, E., Shanafield, M., Hammond, J. C., Sefton, C., Leigh, C., & Datry, T. (2021). Classification and trends in intermittent river flow regimes in Australia, northwestern Europe and USA: A global perspective. *Journal of Hydrology*, 597, 126170. <https://doi.org/10.1016/j.jhydrol.2021.126170>
- Seybold, E. C., Bergstrom, A., Jones, C. N., Burgin, A. J., Zipper, S., Godsey, S. E., et al. (2023). How low can you go? Widespread challenges in measuring low stream discharge and a path forward. *Limnology and Oceanography Letters*, 8(6), 804–811. <https://doi.org/10.1002/lol2.10356>
- Shanafield, M., Bourke, S. A., Zimmer, M. A., & Costigan, K. H. (2021). An overview of the hydrology of non-perennial rivers and streams. *WIREs Water*, 8(2), e1504. <https://doi.org/10.1002/wat2.1504>

- Sprenger, M., Llorens, P., Gallart, F., Benettin, P., Allen, S. T., & Latron, J. (2022). Precipitation fate and transport in a Mediterranean catchment through models calibrated on plant and stream water isotope data. *Hydrology and Earth System Sciences*, 26(15), 4093–4107.
<https://doi.org/10.5194/hess-26-4093-2022>
- Sullivan, P. L., Stops, M. W., Macpherson, G. L., Li, L., Hirmas, D. R., & Dodds, W. K. (2019). How landscape heterogeneity governs stream water concentration-discharge behavior in carbonate terrains (Konza Prairie, USA). *Chemical Geology*, 527, 118989.
<https://doi.org/10.1016/j.chemgeo.2018.12.002>
- Sullivan, Pamela L., Zhang, C., Behm, M., Zhang, F., & Macpherson, G. L. (2020). Toward a new conceptual model for groundwater flow in merokarst systems: Insights from multiple geophysical approaches. *Hydrological Processes*, 34(24), 4697–4711.
<https://doi.org/10.1002/hyp.13898>
- Swenson, L. J., Zipper, S., Peterson, D. M., Jones, C. N., Burgin, A. J., Seybold, E., Kirk, M.F., Hatley, C. (2023). Water isotopes and associated scripts for the analysis of water age and source. [Dataset]. Zenodo. <https://doi.org/10.5281/zenodo.7633403>
- The Navigable Waters Protection Rule: Definition of “Waters of the United States.” (2020, April 21). Retrieved from <https://www.federalregister.gov/documents/2020/04/21/2020-02500/the-navigable-waters-protection-rule-definition-of-waters-of-the-united-states>
- Tramblay, Y., Rutkowska, A., Sauquet, E., Sefton, C., Laaha, G., Osuch, M., et al. (2021). Trends in flow intermittence for European rivers. *Hydrological Sciences Journal*, 66(1), 37–49.
<https://doi.org/10.1080/02626667.2020.1849708>
- Tsy-pin, M., & Macpherson, G. L. (2012). The effect of precipitation events on inorganic carbon in soil and shallow groundwater, Konza Prairie LTER Site, NE Kansas, USA. *Applied Geochemistry*, 27(12), 2356–2369. <https://doi.org/10.1016/j.apgeochem.2012.07.008>
- Van Meter, K. J., Van Cappellen, P., & Basu, N. B. (2018). Legacy nitrogen may prevent achievement of water quality goals in the Gulf of Mexico. *Science*, 360(6387), 427–430.
<https://doi.org/10.1126/science.aar4462>
- Vero, S. e., Macpherson, G. I., Sullivan, P. I., Brookfield, A. e., Nippert, J. b., Kirk, M. f., et al. (2018). Developing a Conceptual Framework of Landscape and Hydrology on Tallgrass Prairie:A Critical Zone Approach. *Vadose Zone Journal*, 17(1), 170069. <https://doi.org/10.2136/vzj2017.03.0069>

- Vu, H. M., Shanafield, M., & Batelaan, O. (2018). Flux dynamics at the groundwater-surface water interface in a tropical catchment. *Limnologica*, 68, 36–45.
<https://doi.org/10.1016/j.limno.2017.06.003>
- Walsh, R., & Ward, A. S. (2022). An overview of the evolving jurisdictional scope of the U.S. Clean Water Act for hydrologists. *WIREs Water*, 9(5), e1603. <https://doi.org/10.1002/wat2.1603>
- Ward, A. S., Wade, J., Kelleher, C., & Schewe, R. L. (2023). Clarify jurisdiction of US Clean Water Act. *Science*, 379(6628), 148–148. <https://doi.org/10.1126/science.adf7391>
- Warix, S. R., Godsey, S. E., Lohse, K. A., & Hale, R. L. (2021). Influence of groundwater and topography on stream drying in semi-arid headwater streams. *Hydrological Processes*, 35(5), e14185. <https://doi.org/10.1002/hyp.14185>
- Zarnetske, J. P., Haggerty, R., Wondzell, S. M., & Baker, M. A. (2011). Dynamics of nitrate production and removal as a function of residence time in the hyporheic zone. *Journal of Geophysical Research: Biogeosciences*, 116(G1). <https://doi.org/10.1029/2010JG001356>
- Zimmer, M. A., & McGlynn, B. L. (2017). Bidirectional stream–groundwater flow in response to ephemeral and intermittent streamflow and groundwater seasonality. *Hydrological Processes*, 31(22), 3871–3880. <https://doi.org/10.1002/hyp.11301>
- Zimmer, M. A., & McGlynn, B. L. (2018). Lateral, Vertical, and Longitudinal Source Area Connectivity Drive Runoff and Carbon Export Across Watershed Scales. *Water Resources Research*, 54(3), 1576–1598. <https://doi.org/10.1002/2017WR021718>
- Zimmer, M. A., Burgin, A. J., Kaiser, K., & Hosen, J. (2022). The unknown biogeochemical impacts of drying rivers and streams. *Nature Communications*, 13(1), 7213.
<https://doi.org/10.1038/s41467-022-34903-4>
- Zipper, S., Popescu, I., Compare, K., Zhang, C., & Seybold, E. C. (2022). Alternative stable states and hydrological regime shifts in a large intermittent river. *Environmental Research Letters*, 17(7), 074005. <https://doi.org/10.1088/1748-9326/ac7539>
- Zipper, S. C., Soylu, M. E., Kucharik, C. J., & Loheide II, S. P. (2017). Quantifying indirect groundwater-mediated effects of urbanization on agroecosystem productivity using MODFLOW-AgroIBIS (MAGI), a complete critical zone model. *Ecological Modelling*, 359, 201–219. <https://doi.org/10.1016/j.ecolmodel.2017.06.002>
- Zipper, S. C., Hammond, J. C., Shanafield, M., Zimmer, M., Datry, T., Jones, C. N., et al. (2021). Pervasive changes in stream intermittency across the United States. *Environmental Research Letters*, 16(8), 084033. <https://doi.org/10.1088/1748-9326/ac14ec>



Water Resources Research

Supporting Information for

Changes in water age during dry-down of a non-perennial stream

Logan J. Swenson^{1,2,*}, Sam Zipper¹, Delaney M. Peterson³, C. Nathan Jones³, Amy J. Burgin⁴, Erin Seybold¹, Matthew F. Kirk⁵, Camden Hatley^{1,2}

1. Kansas Geological Survey, University of Kansas

2. Department of Geology, University of Kansas

3. Department of Biological Sciences, University of Alabama

4. Kansas Biological Survey-Center for Ecological Research, University of Kansas

5. Department of Geology, Kansas State University

Corresponding author: loganswenson@ku.edu

Contents of this file

Text S1 and S2

Figures S1 to S8

Introduction

This SI contains a detailed description of our sampling strategy (Text S1), random forest to predict $\delta^{18}\text{O}$ compositions (Text S2), and supplementary figures (Figures S1 to S8).

Text S1. Sampling strategy

The 50 sampling sites in this study were defined to leverage existing long-term data while spanning a range of watershed physiographic and no-flow conditions. In addition to the water isotope samples investigated in this study, these sampling sites were also used for a variety of other samples including microbial and macroinvertebrate communities, other water chemistry parameters, and instrumentation with stream temperature, intermittency, and conductivity (STIC) sensors, and therefore the sampling approach used was meant to balance the competing priorities of these teams, rather than optimize the sampling from a purely isotope-driven perspective.

First, we identified a subset of priority locations that we wanted to ensure were sampled. These priority locations included sites with existing hydrological data including long-term weirs maintained by the Konza LTER network (n=4), existing stream intermittency sensors from other projects (n=10, which included our planned watershed outlet location), locations immediately downstream of a subset of springs identified during field mapping campaigns (n=7), and near unmonitored tributary junctions (n=2). Combined, these priority locations made up 23 of our sampling sites.

For the remaining 27 sites, we distributed sampling sites using a stratified random sampling approach spanning two variables that have previously been shown to influence stream intermittency: topographic wetness index (TWI) and drainage area (Warix et al., 2021). TWI is a unitless physiographic variable that integrates drainage area and local slope, and locations with higher TWI values are locations that may be wetter due to the accumulation of water from upslope areas. To distribute the points randomly, we first discretized the stream network into equally spaced points at 2 m resolution, which matches the resolution of the DEM used to create the stream network map. We then binned these points into 10 bins that had approximately equal width at the lower end of the drainage area distribution, where points were more densely concentrated, and approximately the same number of total stream points at the higher end of the drainage area distribution, where points were less densely concentrated (Figure S1).

To obtain 50 total sampling points spanning a range of TWI and drainage area conditions, we attempted to place 5 sampling sites within each drainage area bin that spanned the range of TWI values within that bin. To accomplish this, for each drainage area bin we split the range of TWI into 5 quantiles, which we refer to here as bin-quantiles. We identified how many priority locations were already within each bin-quantile and randomly selected a point on the stream network within each bin-quantile, ensuring that it was > 100 m from any existing sampling site. If the priority sites included multiple sampling sites within a given bin-quantile, we could not place a sampling site in each of the bin-quantiles, in which case we randomly selected bin-quantiles to reach a total of 5 sampling sites within that drainage area bin. There were 6 bin-quantiles that we were unable to select sampling sites because all points within that bin-quantile were within 100 m of an existing sampling site. These remaining 6 sampling sites were placed by manually inspecting the stream network and identifying substantial gaps. We then made slight adjustments to some of the sampling sites that were randomly located, for example moving the location from downstream to upstream of a road crossing and/or further back from a tributary junction.

The final distribution of the 50 sampling sites with respect to drainage area and TWI is shown in Figure S2 and Figure S3. Figure 1 shows the spatial distribution of the sampling sites within the stream network.

Text S2. Random forest to predict $\delta^{18}\text{O}$ compositions

We developed a random forest model to predict stream $\delta^{18}\text{O}$ compositions and to quantify the factors that most strongly influence $\delta^{18}\text{O}$ during the summer dry-down of the South Fork of Kings Creek (i.e., the synoptic samples only) using the *party* package in R (Hothorn et al., 2006; Strobl et al., 2007; Strobl et al., 2008). Random forest models are particularly well-suited for hydrological prediction due to their ability to handle numerous predictors with potentially nonlinear and interacting relationships, relatively low risk of overfitting, and ease in interpreting the importance of each input variable (Eng et al., 2017; Addor et al., 2018; Miller et al., 2018). We developed a random forest model to predict $\delta^{18}\text{O}$ across all sites and sampling dates using the following predictor variables: day of year (i.e., date of sampling event), flow state (i.e., whether flowing or pooled), water temperature, topographic wetness index, contributing area, burn frequency, elevation, and slope. We then extracted the conditional permutation importance for each predictor variable (Strobl et al., 2008), which accounts for collinearity among other predictors. A higher conditional variable importance indicates that the predictor variable has a greater influence on model predictors for the out-of-bag samples used in model training. Lastly, we calculated the root mean squared error (RMSE) between the predicted $\delta^{18}\text{O}$ and the observed $\delta^{18}\text{O}$ to assess model performance. We found that day of year, flow state, and water temperature were the most influential predictor variables (Figure S6). This further supports our findings that evaporation and a decrease in surface water connectivity are the primary factors influencing stream $\delta^{18}\text{O}$ compositions (see Figure 5 in the main text).

Figures

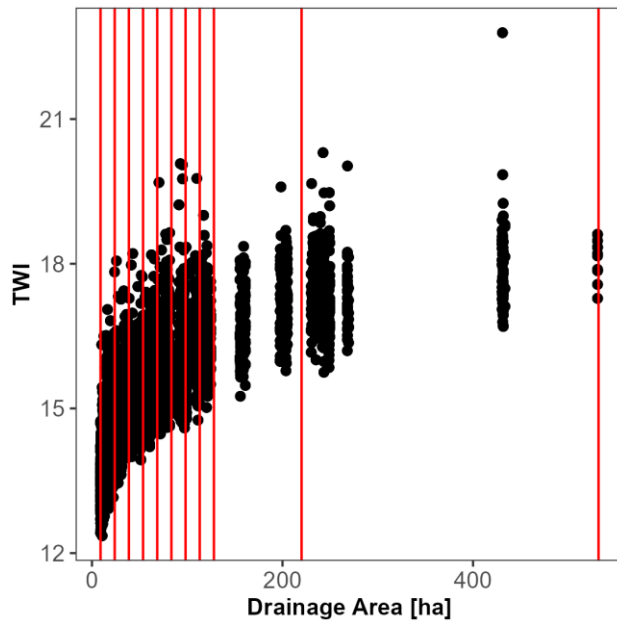


Figure S1. Distribution of drainage area and TWI for all stream network points at the site. The red vertical lines indicate the 10 drainage area groups used to randomly distribute points, and each bin was divided into 5 quantiles based on the TWI distribution.

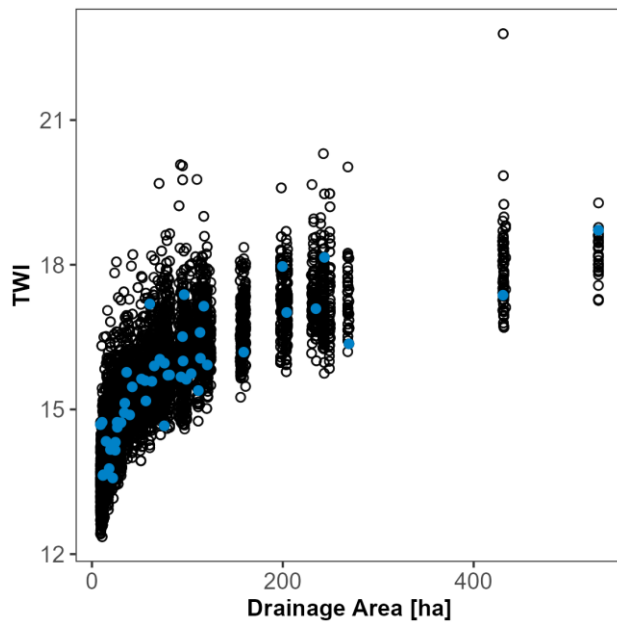


Figure S2. Distribution of drainage area and TWI for sampling sites (blue) and all stream network points (black) at the site.

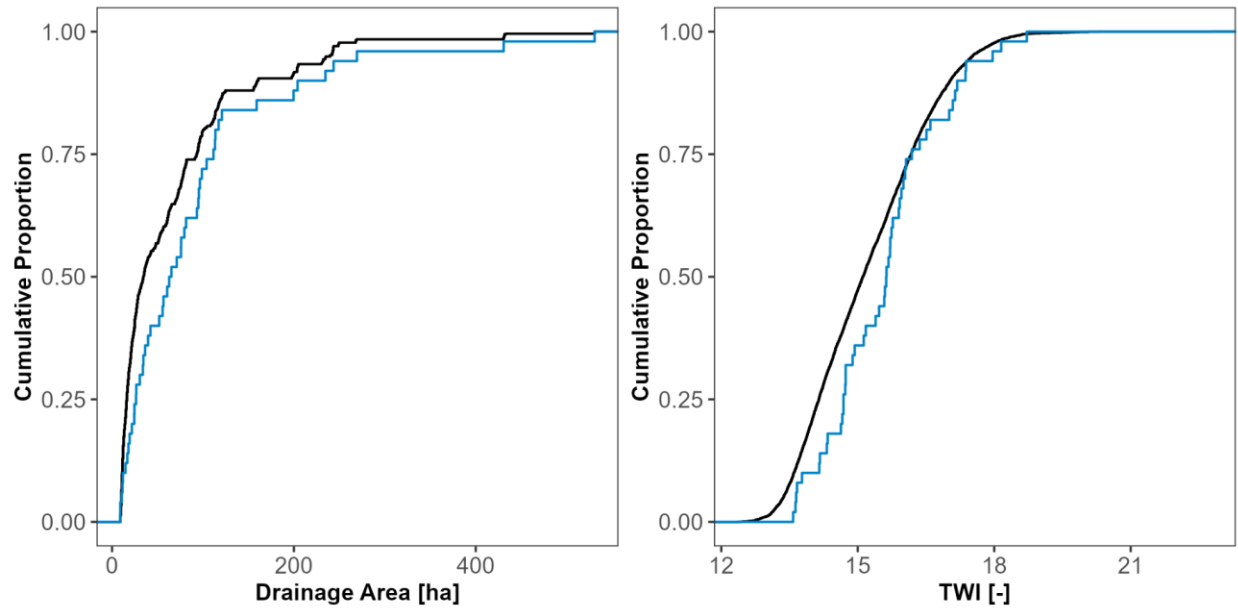


Figure S3. Empirical cumulative distribution functions (ECDFs) of drainage area and TWI for all stream points (black) and sampling sites (blue) for the site.

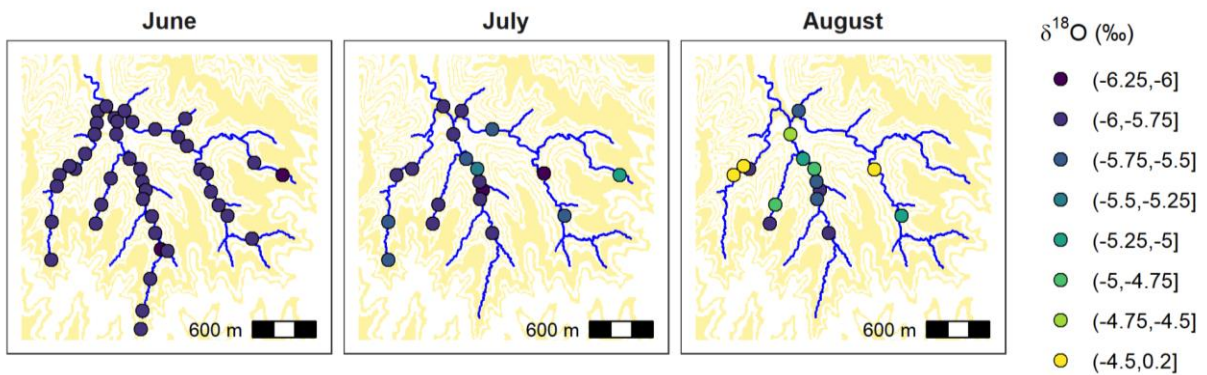


Figure S4. Spatial variation in $\delta^{18}\text{O}$ during the summer dry-down period. The estimated elevations at which limestone units outcrop the watershed are shown as yellow bands. These elevations are based on the average member thickness in the drilling log records at the Konza Prairie.

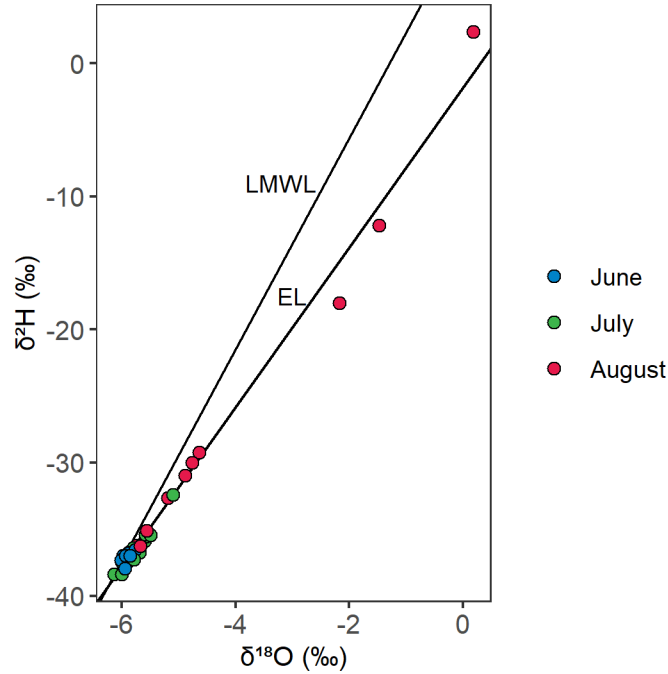


Figure S5. Stream $\delta^{18}\text{O}$ and $\delta^2\text{H}$ in the South Fork of Kings Creek. Shown are the local meteoric water line (LMWL) and the evaporation line (EL). The LMWL ($\delta^2\text{H} = 7.93 \times \delta^{18}\text{O} + 10.28$, $R^2 = 0.97$) is based on a long-term record of precipitation isotopes collected at Konza Prairie by the National Ecological Observatory Network (NEON, 2022).

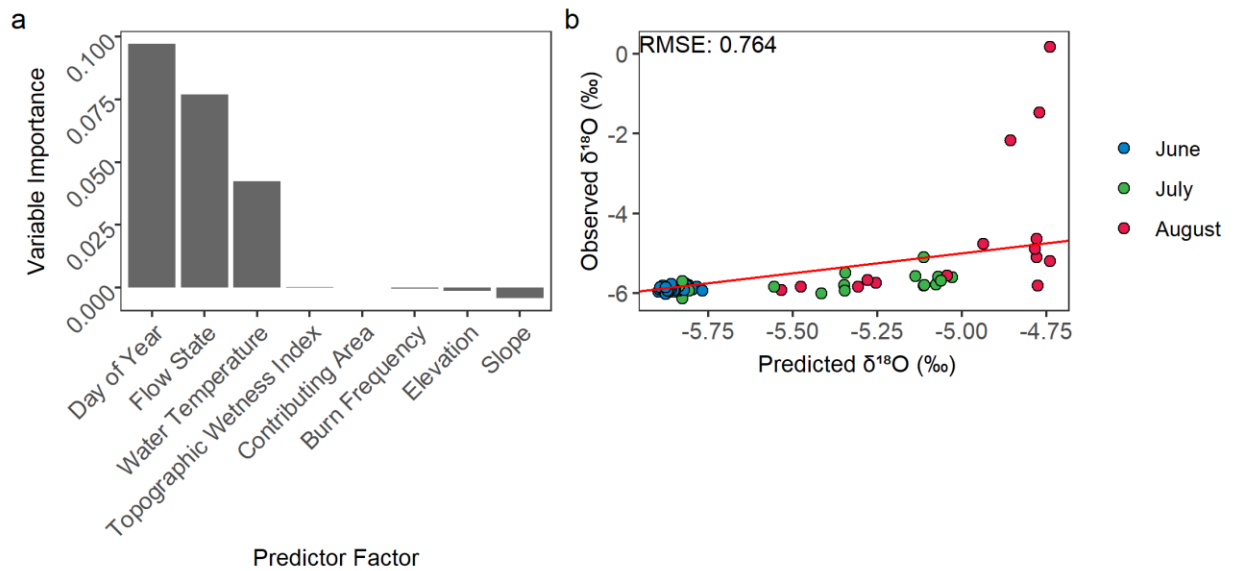


Figure S6. Random forest model to predict $\delta^{18}\text{O}$ in the South Fork of Kings Creek. Shown are (a) predictor factors ordered according to decreasing conditional permutation importance and (b) model fit. The red line shows a 1:1 match between predicted and observed.

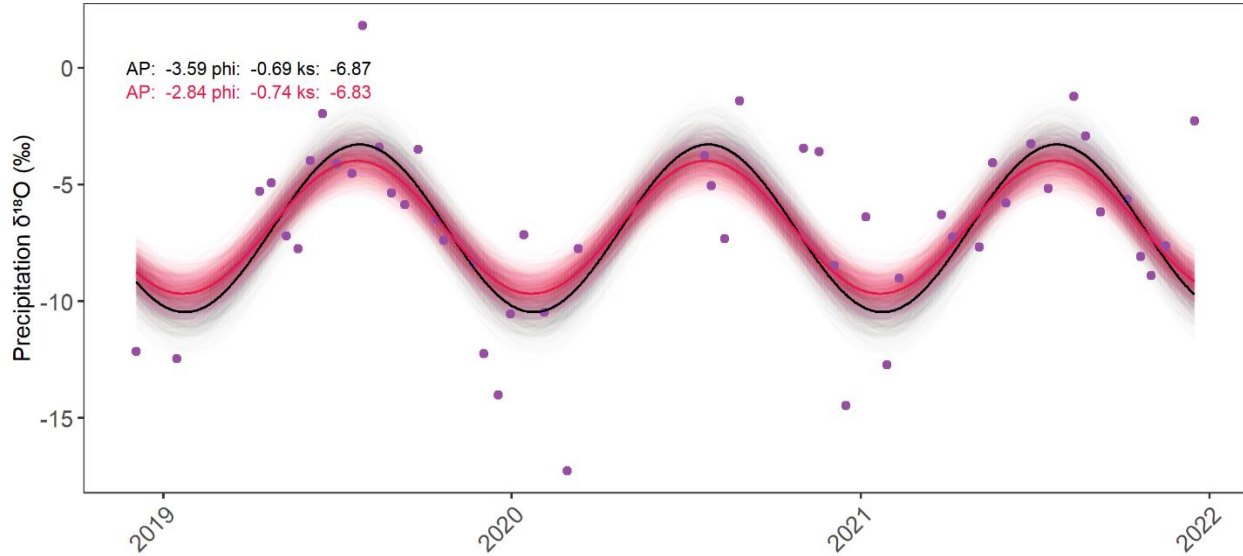


Figure S7. Seasonal $\delta^{18}\text{O}$ model (Eq. 3) fit to precipitation $\delta^{18}\text{O}$ isotopes. The coefficients A_P , φ_P , and k_P were estimated using nonlinear least squares regression with a Gauss-Newton algorithm. The black curve is an unweighted fit, while the red curve is a precipitation amount-weighted fit. Uncertainty was evaluated by sampling A_P , φ_P , and k_P 1,000 times from normal distributions with standard deviations equal to the standard errors on the fitted coefficients.

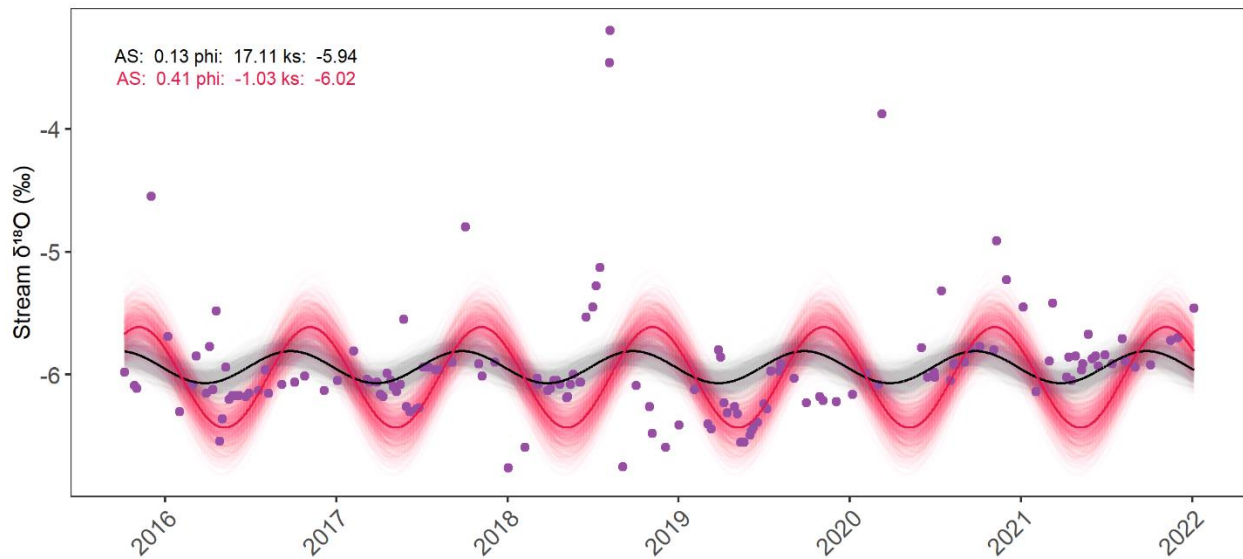


Figure S8. Seasonal $\delta^{18}\text{O}$ model (Eq. 4) fit to stream $\delta^{18}\text{O}$ isotopes. The coefficients A_S , φ_S , and k_S were estimated using nonlinear least squares regression with a Gauss-Newton algorithm. The black curve is an unweighted fit, while the red curve is a flow-weighted fit. Uncertainty was evaluated by sampling A_S , φ_S , and k_S 1,000 times from normal distributions with standard deviations equal to the standard errors on the fitted coefficients.

References

- Addor, N., Nearing, G., Prieto, C., Newman, A. J., Le Vine, N., & Clark, M. P. (2018). A Ranking of Hydrological Signatures Based on Their Predictability in Space. *Water Resources Research*, 54(11), 8792–8812. <https://doi.org/10.1029/2018WR022606>
- Eng, K., Grantham, T. E., Carlisle, D. M., & Wolock, D. M. (2017). Predictability and selection of hydrologic metrics in riverine ecohydrology. *Freshwater Science*, 36(4), 915–926. <https://doi.org/10.1086/694912>
- Hothorn, T., Bühlmann, P., Dudoit, S., Molinaro, A., & Van Der Laan, M. J. (2006). Survival ensembles. *Biostatistics*, 7(3), 355–373. <https://doi.org/10.1093/biostatistics/kxj011>
- Lutz, S. R., Krieg, R., Müller, C., Zink, M., Knöller, K., Samaniego, L., & Merz, R. (2018). Spatial Patterns of Water Age: Using Young Water Fractions to Improve the Characterization of Transit Times in Contrasting Catchments. *Water Resources Research*, 54(7), 4767–4784. <https://doi.org/10.1029/2017WR022216>
- Miller, M. P., Carlisle, D. M., Wolock, D. M., & Wiczorek, M. (2018). A Database of Natural Monthly Streamflow Estimates from 1950 to 2015 for the Conterminous United States. *JAWRA Journal of the American Water Resources Association*, 54(6), 1258–1269. <https://doi.org/10.1111/1752-1688.12685>
- Strobl, C., Boulesteix, A.-L., Zeileis, A., & Hothorn, T. (2007). Bias in random forest variable importance measures: Illustrations, sources and a solution. *BMC Bioinformatics*, 8(1), 25. <https://doi.org/10.1186/1471-2105-8-25>
- Strobl, C., Boulesteix, A.-L., Kneib, T., Augustin, T., & Zeileis, A. (2008). Conditional variable importance for random forests. *BMC Bioinformatics*, 9(1), 307. <https://doi.org/10.1186/1471-2105-9-307>
- Warix, S. R., Godsey, S. E., Lohse, K. A., & Hale, R. L. (2021). Influence of groundwater and topography on stream drying in semi-arid headwater streams. *Hydrological Processes*, 35(5), e14185. <https://doi.org/10.1002/hyp.14185>